Hybrid Humanoid Robot

A Technical Report submitted to the Department of Mechanical and Aerospace Engineering

Presented to the Faculty of the School of Engineering and Applied Science

University of Virginia • Charlottesville, Virginia

In Partial Fulfillment of the Requirements for the Degree

Bachelor of Science, School of Engineering

Morgan Carr

Spring, 2025

Technical Project Team Members

Ekow Daniels

Jack de Bruyn Kops

Amelia Dinsmore

Colin Halligan

Patrick Lam

Carson Peters

Dorian Thomson

On my honor as a University Student, I have neither given nor received unauthorized aid on this assignment as defined by the Honor Guidelines for Thesis-Related Assignments

Pawandeep Matharu, Department of Mechanical and Aerospace Engineering

Introduction

The use of robotics for military applications has significantly expanded since the early 20th century. What started as a way to automate calculations and reduce the complexity of processes has now evolved to a point where the military is investing in robotic solutions to put humans out of harm's way. Our project follows this theme by aiming to reduce the number of sailors required to operate the underside of an aircraft carrier on a day-to-day basis by creating a hybrid humanoid robot capable of navigating the obstacles and terrain of an aircraft carrier's interior while doing various basic maintenance operations. Being sponsored by the Navy, the project's primary focus is to develop a lightweight, cost-effective robot capable of transforming elements of its limbs to navigate various environments.

To better understand the objectives and goals of this project, it is important to understand the terrain the designed robot must navigate. Per the project requirements given by the Navy, the designed robot must be capable of scaling a 63-degree inclined ladder that is commonly found on aircraft carriers (Fig. 1). Additionally, the robot must be capable of transforming from an upright, bipedal humanoid robot into a quadrupedal-mobile robot that can swiftly travel down long aircraft carrier hallways on sets of wheels (Fig. 2). These requirements demand a solution where the limbs of the final robot can transform, making the final robot a Hybrid Humanoid Robot.

The idea of a hybrid humanoid robot is an advancement in robotics in several ways. The current state of humanoid robotics forces engineers to make a tradeoff, choosing between either mobility or functionality. By creating a hybrid robot capable of moving quickly on flat terrain and capable of climbing a steep set of stairs, the hybrid robot design can achieve what no other commercially available robot can do. By creating a robot with these capabilities, we can reduce

the number of sailors required to operate an aircraft carrier, removing sailors from potentially dangerous jobs. This technology also opens the door for fully autonomous aircraft carriers and proves that elements of a concept that were thought to be too challenging can be overcome.


Figures 1 and 2: A 63-degree ladder typical on an aircraft carrier and a long stretch of aircraft carrier hallway

T

It is also important to note that as the semester progressed, the scope of the project that our group was assigned was reduced to create a more achievable goal for the end of the year. At the beginning of the semester, we were tasked with designing and developing the entire robot, from the transforming limbs to the frame and the electronics. This list was reduced so that our advisor would create a rudimentary but working prototype for the transforming limbs, and our team would design and manufacture the remainder of the robot. This reduction has led to an increase in focus on frame design that has resulted in a more practical and tested design.

Research

Current advancements in robotics have led to the development of robots capable of navigating complex terrain. For example, Boston Dynamics' Atlas robot was designed for challenging environments and has demonstrated impressive agility and balance, mimicking human-like mobility (Boston Dynamics, 2024). Honda also developed the ASIMO (Advances Step in Innovative Mobility), which was designed to assist with tasks like walking, running, and climbing stairs (ASIMO, 2024). It can also interact with people using voice and gesture recognition. Another example is the Shipboard Autonomous Fire Fighting Robot (SAFFIR), designed to navigate tight and uneven spaces in naval vessels (US Navy, 2021).

There are several cost-effective options that we used as sources of inspiration throughout the design process. The Unitree humanoid robot and Ascento Pro were the two major sources of inspiration we drew from during the initial design process. The Unitree G1 is a commercially available humanoid robot that is lightweight and highly mobile (Unitree, 2024). Released this year, it proves that humanoid robotics is very much still under development and that effective and mobile solutions can be created at a low cost. We referenced the proportions and degrees of freedom for the rotation of limbs from the G1. The G1 is lightweight for a humanoid robot at 35 kg, but our robot needs to be much lighter. The Ascento Pro was also used as inspiration because of its effective use of wheels (Ascento Robotics, 2024). Having wheels attached to the legs gives it the ability to climb steps but also move very quickly. The mobility while rolling is something that we drew inspiration from and wanted to emulate in our design.

Overall, there were lots of examples of humanoid robots we researched while preparing for and designing our robot. We referenced these robots to learn about the way they moved and the systems they employed to achieve design objectives that we identified were similar to ours.

We wanted to find a way to combine the upright ability of the Unitree G1 with the rolling mobility of the Ascento Pro.

Ideation

Leg Subteam -

When deciding the final design our team wanted to pursue concerning the transforming wheel-to-foot, we first brainstormed a list of 10 preliminary concepts (Fig. 3). These concepts ranged from highly achievable to wildly complex, but the goal was to identify a series of design attributes that would create a design that could achieve each of the elements the objectives required of the final design. The designs then underwent a selection and screening process that helped identify which design elements achieved the desired objectives the best.

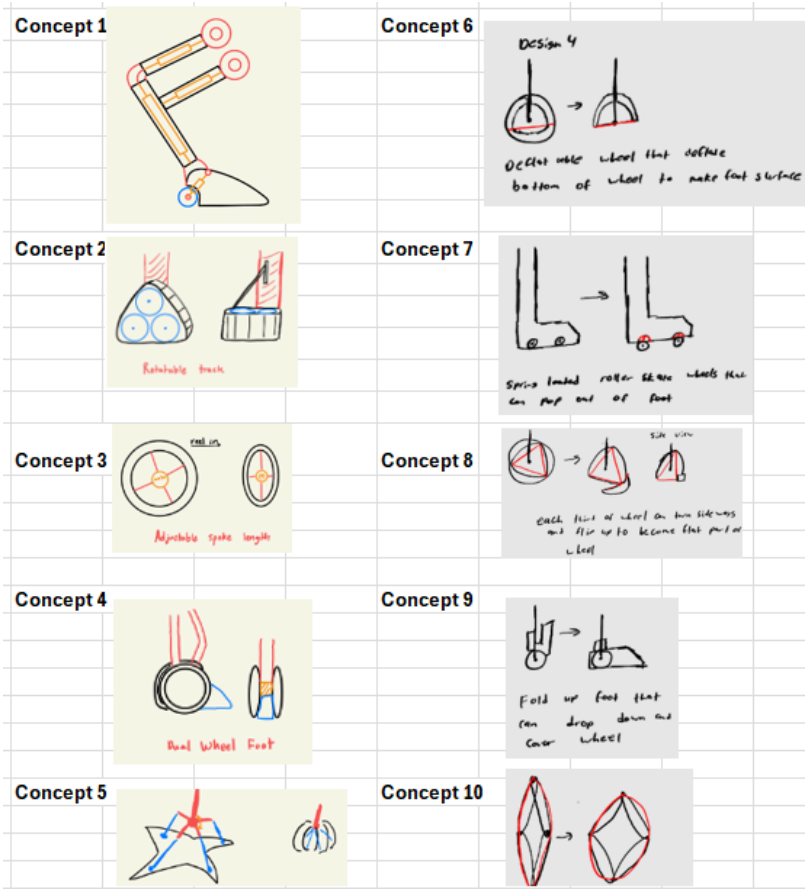

Fig. 3: A list of transforming wheel-to-foot concepts

Arm Subteam -

The initial plan for the arms was also to include a transformable component, this time acting as a wheel-to-hand mechanism. We created 10 conceptual ideas for the limb (Fig. 4), then proceeded to select and screen our concepts, using criteria that we thought fit our design goals.

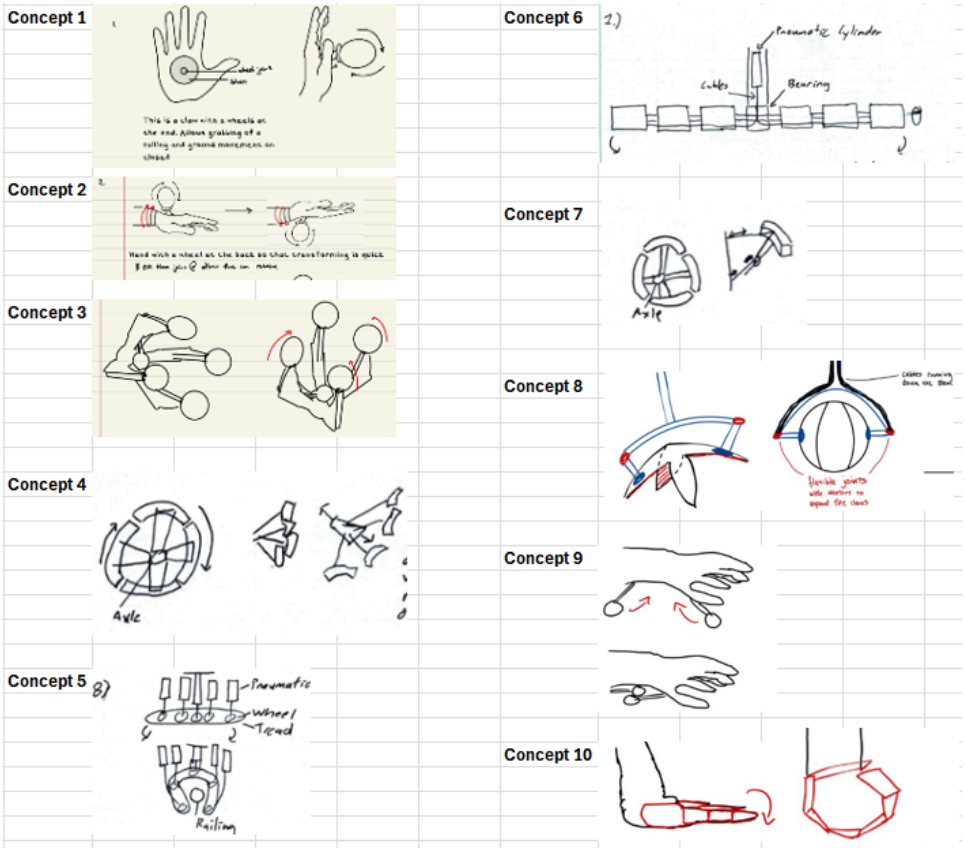

Fig. 4: A list of transforming wheel-to-hand concepts

Torso and Joints Subteam -

For the torso, we originally came up with 10 initial designs, shown in Figure 5. These designs all had a chosen torso shape, an aspect of rotation for the “waist”, and some had the ability to tilt the torso left and right. We selected criteria that fit our design goals and then screened the initial ten ideas to determine what design elements we wanted to move forward with.

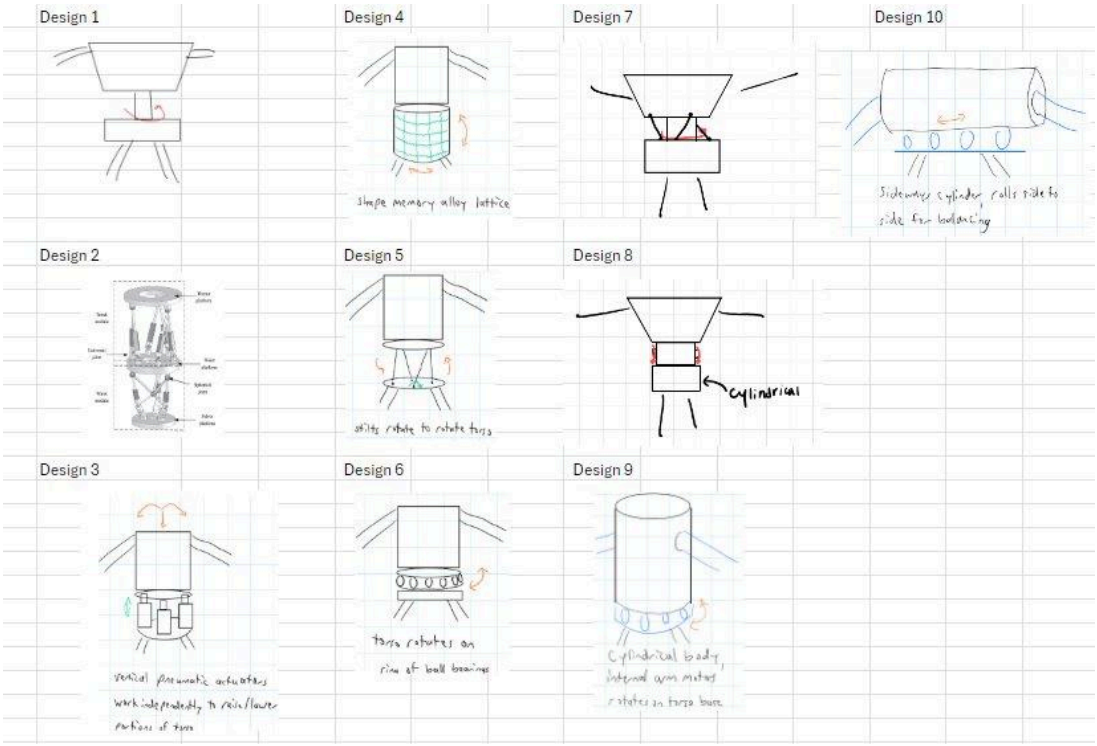

Fig. 5: Initial Torso Design Concepts

For the shoulder joint component, we had to create a bracket that would fit 3 Dynamixel motors with aligned centers of rotation (Fig. 6). This was to allow for better movement of the arms as a spherical shoulder allows for direct changes to pitch, roll, and yaw when adjusting each motor that comprises the shoulder. This joint was added after the project scope was changed so it didn't go through the traditional ideation phase.

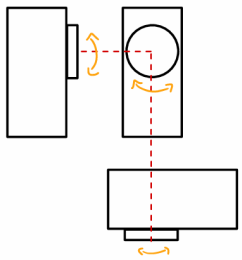

Fig. 6: Shoulder Degrees of Freedom

Selection and Screening

Leg Subteam -

After creating a list of the 10 design ideas whose traits we believed could best achieve the required design goals, we made a list of criteria that best represented the objectives of the required design (Fig. 7). Using these criteria, each of the 10 designs was evaluated, the three highest scorers were dissected, and their successful elements were combined to create 5 new design ideas which were evaluated using the same criteria and the most successful would be developed.

Concept	1	2	3	4	5	6	7	8	9	10
Smoothness	0	+	+	-	0	0	0	+	0	-
Rotatability	0	0	0	+	+	-	-	0	-	0
Size of wheel	0	+	+	+	+	+	-	+	0	+
Mountability	0	-	-	-	-	+	+	-	-	+
Reliability	0	+	-	0	-	0	+	-	+	-
Durability	0	+	0	0	0	0	-	0	0	-
Time to transform	0	-	-	+	-	0	+	0	+	0
Traction	0	+	-	-	-	0	-	+	0	-
Total Plus	0	5	2	3	2	2	3	3	2	2
Total Minus	0	2	4	3	4	1	4	2	2	4
Total	0	3	-2	0	-2	1	-1	1	0	-2
Rank	4	1	9	5	10	2	7	3	6	8
Move Forward with:		2				6		8		

Fig. 7: Scoring chart for transforming wheel-to-foot designs

Following the first round of scoring, designs 2, 6, and 8 were found to have the most beneficial design. These designs were then reworked into new concepts and evaluated using the same set of criteria. When evaluating the new designs, each design was rated 1 through 5 for each of the criteria instead of the plus-minus system seen in Fig. 7 (Fig. 8). Each of the design objectives was also given a weight to demonstrate how important it was to the final design. The design goals that were given the highest weight for the wheel-to-foot design were the smoothness

of rotation, mountability, and reliability. These objectives were weighted the highest because of the nature of the project having a military application. The customer being the US Navy, the designed mechanism needs to be able to reliably work in less-than-perfect conditions. That means these factors are crucial to the success of our overall design. It was found that our 5th design (Fig. 9) was the most successful and should be pursued. It should also be noted that despite the reduction of the scope of the project, our project advisor did choose to pursue this design idea.

Concept	Weight	1	Weighted 1	2	Weighted 2	3	Weighted 3	4	Weighted 4	5	Weighted 5
Smoothness	0.2	3	0.6	3	0.6	3	1	5	1	4	0.8
Rotatability	0.05	5	0.25	2	0.1	2	0.15	3	0.15	3	0.15
Size of wheel	0.1	3	0.3	4	0.4	5	0.4	4	0.4	5	0.5
Mountability	0.2	1	0.2	4	0.8	3	0.4	2	0.4	2	0.4
Reliability	0.2	2	0.4	3	0.6	3	0.6	3	0.6	3	0.6
Durability	0.12	2	0.24	3	0.36	2	0.24	2	0.24	3	0.36
Time to transform	0.05	2	0.1	3	0.15	3	0.2	4	0.2	3	0.15
Traction	0.08	3	0.24	4	0.32	5	0.32	4	0.32	5	0.4
Sum		21		26		26		27		28	
Rating			2.33		3.33		3.31		3.31		3.36
Rank			5		2		4		3		1
Move Forward with:											5

Fig 8: Second concept selection chart which was used to select the final design for the transforming wheel-to-foot

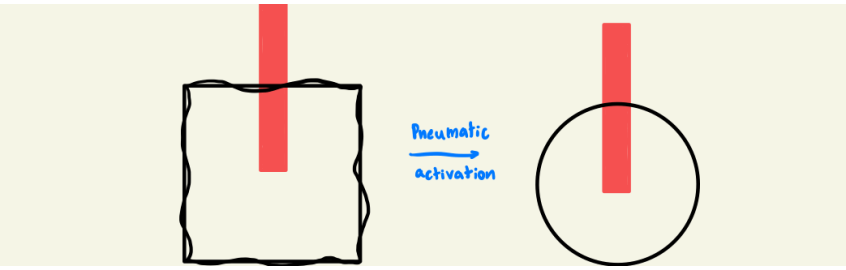

Fig 9: Final selected concept of a pneumatically activated wheel-to-foot design

Arm Subteam -

Following a slightly altered scoring system than the leg subteam, and using concept 8 as the base we produced the scoring chart seen in Fig. 10.

	Concept									
Criteria	**8**	**1**	**2**	**3**	**4**	**5**	**6**	**7**	**9**	**10**
Shapeshifting	0	-3	-3	-3	0	0	0	0	-1	0
Novel	0	-3	-1	0	1	2	2	2	-1	0
Weight	0	-2	-2	-3	3	-3	-2	-3	-2	0
Simplicity	0	3	3	2	0	-1	-2	-2	2	-2
Connections	0	3	3	3	1	-1	-3	-2	1	-2
Size	0	-3	-3	-3	0	-3	-3	-3	-2	-1
Function as Wheel	0	0	0	2	0	-2	-2	-2	-2	-3
Function as Hand	0	1	3	-1	-2	0	-1	0	1	-1
Total Sum	0	-4	0	-3	3	-8	-11	-10	-4	-9
Rank	2	4	2	3	1	5	8	7	4	6
Move Forward With	8		2		4					

Fig. 10: Scoring chart for wheel-to-hand designs

These were the key selection criteria that we based our conceptual designs on. As a transformable mechanism, a reliable shapeshifting process was necessary. Weight and size were also key factors to consider to meet project requirements, and we did not want anything too complex, with minimal moving parts. Additionally, our part had to function as both a wheel and a hand to allow for varied movements. These weights were reflected in the updated scoring chart that was used to evaluate the second set of designs (Fig. 11).

		Unweighted Scores			Weighted Scores		
Selection Criteria	**Weightings (%)**	**Design 8**	**Design 4**	**Design 2**	**Design 8**	**Design 4**	**Design 2**
Shapeshifting	20	5	5	1	1	1	0.2
Weight	15	4	3.5	2	0.6	0.525	0.3
Ease of Manufacture	5	2	3	1	0.1	0.15	0.05
Connections	10	2	2.5	4	0.2	0.25	0.4
Function as Wheel	25	4	4	4	1	1	1
Function as Hand	25	3.5	3.5	3	0.875	0.875	0.75
Sum					3.775	3.8	2.7
Rating					75.5	76	54
Rank					2	1	3

Fig. 11: Ranking chart for wheel-to-hand designs

Concept 4 ended up with the highest ranking with 8 following close behind. However, as mentioned in the introduction, our instructor constructed this wheel-to-hand mechanism differently - with the use of pneumatics - due to the scope of the project being reduced.

Torso and Joints Subteam -

Based on the initial torso designs, we created a list of criteria, similar to the other subteams, that best fit the design objectives for the torso. We evaluated our designs using the scoring chart below (Figure 12). We used design 1 as a base design and then determined if the following designs were better, worse, or even for each criterion. We selected the three top-scoring designs to move forward with.

Criteria	1	2	3	4	5	6	7	8	9	10
Stability	0	-1	1	-1	-1	1	0	0	1	1
Lightweight	0	-1	0	1	1	0	0	0	0	0
Ease of control	0	-1	0	0	-1	1	0	0	0	0
Manufacturing Ease	0	-1	-1	-1	-1	0	-1	0	0	0
Motor Usage	0	-1	1	1	-1	0	0	0	0	0
Ease of assembly	0	-1	-1	-1	-1	0	-1	0	0	0
Production cost	0	-1	-1	-1	0	0	0	0	0	0
Durability	0	-1	1	-1	0	1	0	0	1	1
Space Optimization	0	-1	0	-1	0	1	0	0	1	1
Maintenance	0	-1	0	-1	0	0	0	0	0	0
Simplicity	0	-1	0	-1	-1	0	-1	0	0	0
Total Plus	0	0	3	2	1	4	0	0	3	3
Total Minus	0	-11	-3	-8	-6	0	-3	0	0	0
Net Score	0	-11	0	-6	-5	4	-3	0	3	3
Rank	4	10	6	9	8	1	7	5	2	3

Fig. 12: Scoring Chart for Torso Designs

The three designs we continued to develop were 1, 6, and 8. We determined which elements we liked from each of the three designs and used those to create five new concepts. The simplicity of design number one was preferred as it was easy to design and manufacture as well as lightweight, however, this design didn't allow the robot to bend forward, which is necessary for the project objectives. Design six was more stable and similarly simple to design, but had the

same issue as design number one. Design eight can bend forward, however it doesn't allow for individual movement of the robot's hips. We ranked our modified designs using the chart in Figure 13, which has the same criteria but is weighted to ensure the design we proceed with meets the most important criteria. The most important criterion for the torso design is for it to be lightweight. With our robot performing dual functions while moving upright and bent over, the torso must be light enough that it does not cause the robot to topple over. Additionally, it needs to be stable as we do not currently have a balancing mechanism in our overall design, and the torso needs to be able to support the weight of the arms and remain stable. Our subteam moved forward with design one (Fig. 14). Due to the simplicity of the design, we can make the torso very lightweight and the individual hip motors allow for a wider range of movements. Later in the design process, we decided to incorporate a rotational element into the torso, doing so through a rod that runs through the torso's body and connects to a bar that separates the torso from the hips.

Concept	Weight	1	Weighted 1	2	Weighted 2	3	Weighted 3	4	Weighted 4
Stability	0.2	3	0.6	3	0.6	3	0.6	4	0.8
Lightweight	0.25	5	1.25	3	0.75	4	1	4	1
Ease of control	0.1	4	0.4	4	0.4	4	0.4	4	0.4
Manufacturing Ease	0.1	5	0.5	3	0.3	4	0.4	3	0.3
Motor Usage	0.05	4	0.2	4	0.2	4	0.2	4	0.2
Ease of assembly	0.05	5	0.25	4	0.2	4	0.2	4	0.2
Production cost	0.05	4	0.2	4	0.2	4	0.2	4	0.2
Durability	0.05	4	0.2	4	0.2	4	0.2	4	0.2
Space Optimization	0.1	4	0.4	4	0.4	4	0.4	4	0.4
Sum			4		3.25		3.6		3.7
Rank			1		4		3		2
Move Forward With			1						

Fig. 13: Ranking Chart for Torso Design

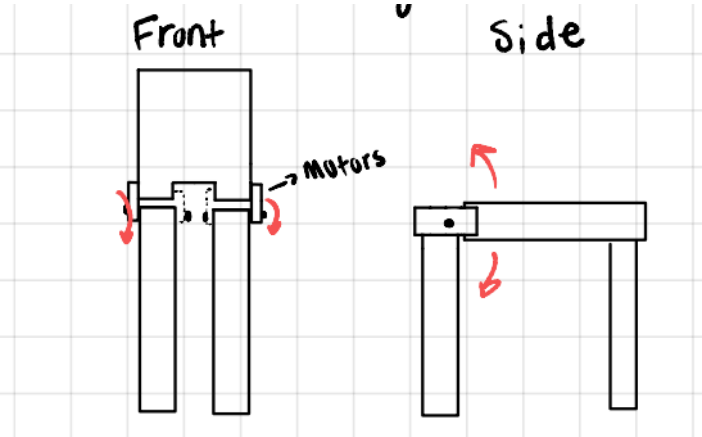

Fig. 14: Final Torso Design

Specifications and Idea Development

When creating the original specifications for the robot, we used a human with a height of about 5 foot 6 inches to base our leg and arm lengths. This led to a robot with leg lengths (with feet and hips) of 41 inches (Fig. 15). It should be noted that the head and neck lengths that would usually be factored into the height were split between the torso and legs in a ratio of 1:2. This initial leg design had limited degrees of freedom, and it was found that the number of degrees of freedom needed to be increased in the final design. The final arm design was also intentionally long to create an increased working reach. This design was thought to benefit the functionality and balance of the robot given the robot's shorter overall height, but our advisor determined the length of these arms was too long and thus too heavy for the motors to maneuver effectively. The final wingspan needed to be reduced from the 96 inches it was originally designed at. Finally, the torso design was too large and added too much weight. We knew when we designed the torso that there would need to be FEA to remove some of the weight, but it was also found that the overall shape was too large. When compared to the team from last year's design, it was roughly twice the volume for the same amount of electronics. This size increased the height of the center of mass unnecessarily and needed to be reduced in the final design.

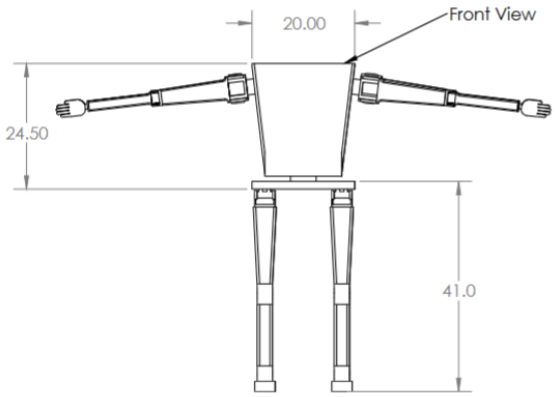

Fig 15: Initial robot basic dimensions and design

To gain a better perspective on the problem and to improve upon the initial design, we used a combination of using our advisor, reviewing the documentation from last year's team, and redefining the problem in better terms. Once the scope of the project was reduced, we approached our advisor with more concrete design questions. The biggest design challenge we identified was deciding the degrees of freedom we needed to include. Mainly, we sought guidance on which degrees of freedom we should include to maximize mobility while reducing weight. We reviewed the previous team's documentation to learn how they connected motors in series to create these degrees of freedom.

Deciding on the degrees of freedom was essential to create a robot capable of walking, climbing, and transforming into quadrupedal form. The final degrees of freedom were decided based on the goal of optimizing balance and maintaining simplistic human-like motion (Fig. 16). Balance was achieved by including three major degrees of freedom. The first one is the extra degree of freedom in the ankle. Being able to shift the angle of the foot allows the robot to level itself on a variety of sloped surfaces. The second degree of freedom critical for balance is in the hip. The degree of freedom that allows the legs to kick out parallel to the hips allows for the

readjustment of individual legs while walking or rotating. The final degree of freedom that increases balance is the third degree of freedom in the shoulder. While you could remove a degree of freedom from the shoulder and have the same working ability due to the degree of freedom in the elbow, the added degree of freedom gives the robot the ability to adjust its arms when it is off balance. With the degrees of freedom decided, the general motor layout and structure of the robot could be decided. The only exception to this was deciding what the expected forces were in each of the limbs to determine how many motors may be needed to support that weight.

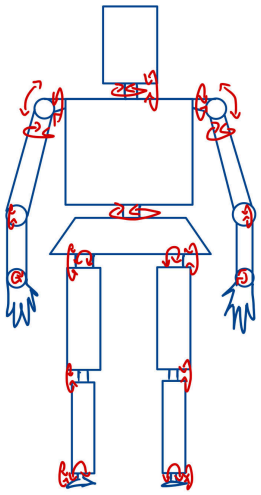

Fig. 16: Final Degrees of Freedom

After the degrees of freedom were decided, we reviewed last year's team's documentation to learn what did and did not work concerning weight reduction and motor strength. The greatest challenge they had with the project was reducing the weight of their robot so the motors could support the full weight of the robot. They used an aluminum frame that had been optimized with CNC, but their overall weight was still too heavy and the motors could not effectively move the limbs or support the body. Their factor of safety was also extremely high, which led us to make the design choice to use ABS to create the majority of our components

while the high-torque-bearing components can be made out of aluminum to add strength; the first iteration will be tested using ABS due to ease of manufacturing though. Finally, the problem was redefined so that the goals of our design were better understood. This included defining the motions needed to transform from bipedal walking to quadrupedal rolling and defining load cases during these motions. This allowed us to design components that could bear the loads from movement, ensuring no components experienced too great of stress (Fig. 19). The formulas used to find these values were found by doing basic physical modeling seen in Figures 17 and 18.

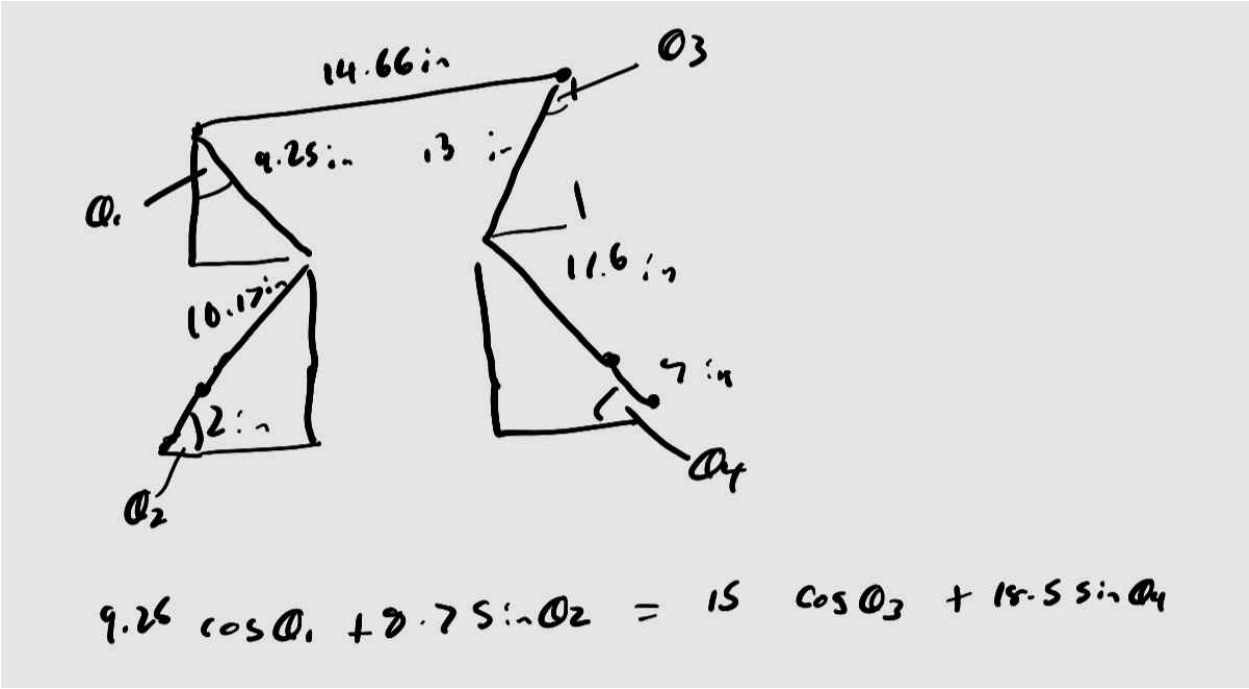

Fig. 17: Calculation to find angles for the robot in quadrupedal mode (values were changed later)

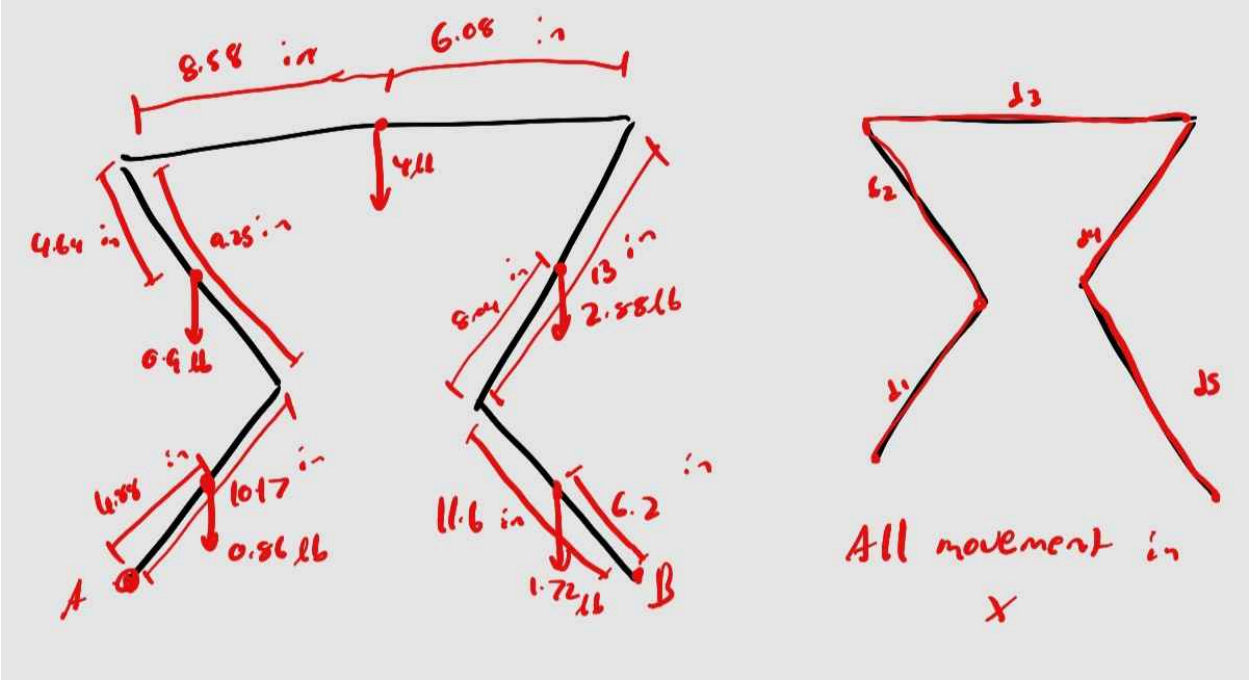

Fig.18: Weight distribution for quadrupedal mode

Theta 1 (Degrees)	Theta 2	Theta 3	Theta 4			Chosen Theta 1	Chosen Theta 3							
1	55	8.533014271	20			47	40.29							
2		8.657638482												
3		8.861439879				Weights (lbm/lbf)							Rb (lbf) (at legs)	Ra (lbf) (at arms)
4		9.139106111				Forearm	0.86	d1	5.833272			Combined	4.249383373	6.110616627
5		9.484128909				Bicep	0.9	d2	-0.93175			At each	2.124691687	3.055308313
6		9.889432744				Torso	4	d3	13.72825					
7		10.34790382				Quad	2.88	d4	5.321714					
8		10.85276891				Calf	1.72	d5	16.22215					
9		11.39782365				Total	10.36							
10		11.9775384				Arms + Torso	5.76							
11		12.58707797												
12		13.22226859				Lengths (in)								
13		13.879537				Forearm	10.17							
14		14.55583875				Bicep	9.25							
15		15.24858578				Torso	14.66							
16		15.95557877				Quad	13							
17		16.6749469				Calf	11.6							
18		17.40509553												
19		18.14466178				CoM (y)								
20		18.89247704				Forearm	4.88							
21		19.64753567				Bicep	4.64							
22		20.40896902				Torso	6.08							
23		21.17602373				Quad	8.04							
24		21.94804382				Calf	6.2							
25		22.72445574												
26		23.50475593												
27		24.2885005												

Fig. 19: Excel calculations done to find a rough estimate of the reaction force at each limb while the robot is in quadrupedal mode

These intermediate adjustments allowed us to create a final design with specifications that meet our design objectives (Figure 20). The final weight of the robot is 27 pounds with a

height of 54 inches and a shoulder width of 19 inches. The broad final specifications of the leg are that the leg has a length of 37.6 inches and a weight, without the foot, of 4.8 pounds (Fig. 21). Physiologically, the average man's leg length is about 34 inches which, when considering the length of the average hip height, comes to roughly the same total length as our designed leg. The weight of the leg, being 4.8 pounds, is also extremely lightweight as the total robot weight must be kept under 33 pounds (reduced from the 45-pound weight the previous year).

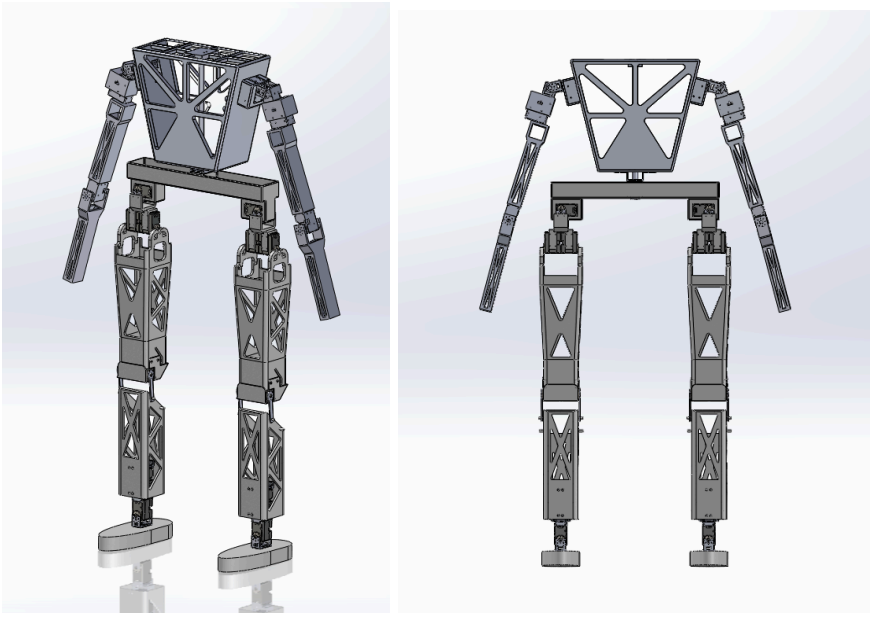

Figure 20: Final robot design

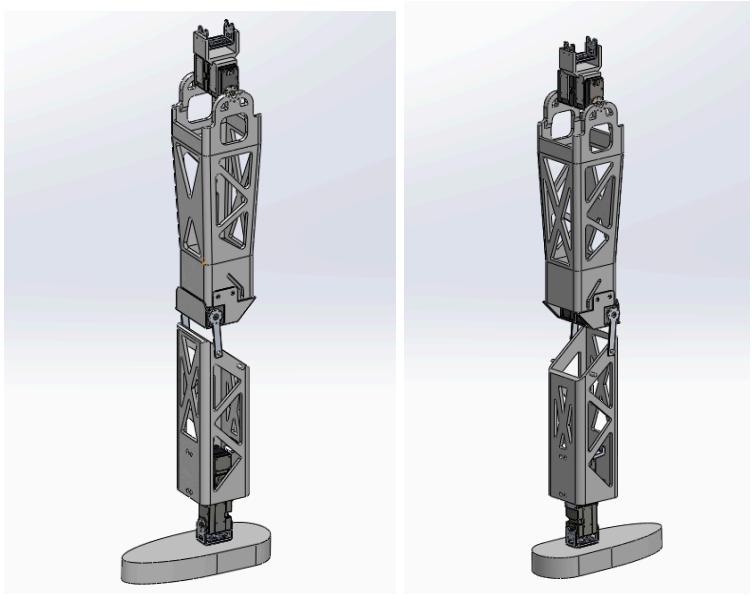

Fig 21: Final leg assembly

The leg was created piece by piece and was designed to better emulate the dimensions of an average adult male leg. The knee assembly was designed first to ensure the task of being able to walk up the 63-degree ladder was possible. To allow for the torque required to lift the entire body when stepping (with assistance from the arms) two motors were placed in the knee. The connections between the calf and knee were also critical to ensuring the knee could make this motion. A damper (not pictured) was found to run between the back of the knee and the top of the calf to act as a hamstring. This damper provides stability when the leg is raised and rested. A channel was added in the connection to the quad to allow a dual damper system to slide via a pin where the lengths are optimized so that when the leg is completely down, the damper is at almost maximum extended length. This creates the resting stability needed to stand upright. The calf is also connected by a rotating motor mount that is the minimum length to achieve the degree of rotation we desire when walking up the ladder.

A two-degree of freedom ankle assembly is also embedded in the lower calf and connected to the foot. This assembly connects to the calf via two custom brackets that strategically place the assembly off-center so the foot can rotate more in one direction than the other. The leg is connected to the hip via a set of two motors run in series connected by a bracket. Last year's team used only one motor for this motion, and while it was strong enough to lift the leg, it was not strong enough to support the robot, so an extra motor was added to increase the torque capability. Finally, the leg was optimized so that its weight was minimized while the structural integrity was maintained. To optimize each of the major components, FEA was performed using load cases similar to expected real-life load cases. When the calf was initially tested, it was found to be nowhere near yielding (Fig. 22). The load case for the first calf FEA

test was 30 pounds placed directly downward on the connection pins (Fig. 23). The calf experienced stress at the pin connections, but the stress was far less than the yield strength of ABS. The second load case was to mimic the stress when the calf is being used as a pivot point during leg rotation and while walking up the ladder. This case was identified to be a likely point of failure due to a combination of stresses and the whole weight of the robot on an angled leg. The loading was 22 pounds applied to the back of the calf with 10 lbf-in applied at each corner of the calf (Fig. 24). The stress experienced was 10 times less than the yield stress of ABS, creating a large factor of safety.

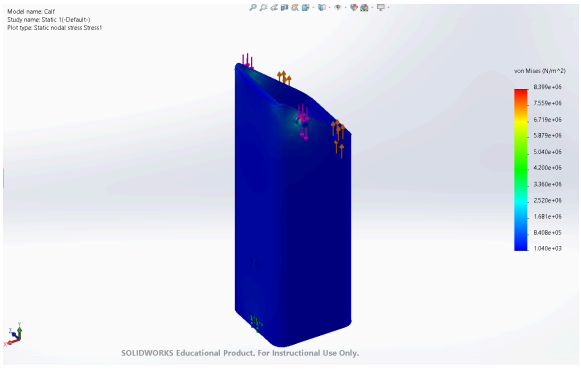

Fig. 22: Initial calf FEA

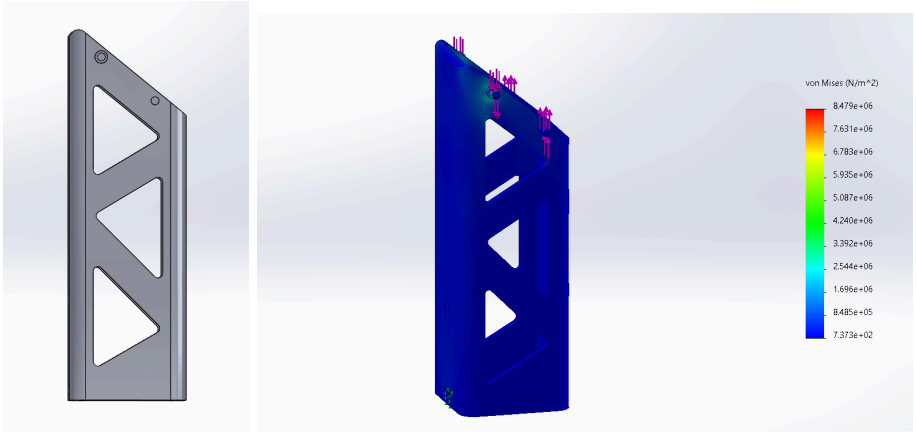

Fig. 23: Optimized calf and first load case FEA

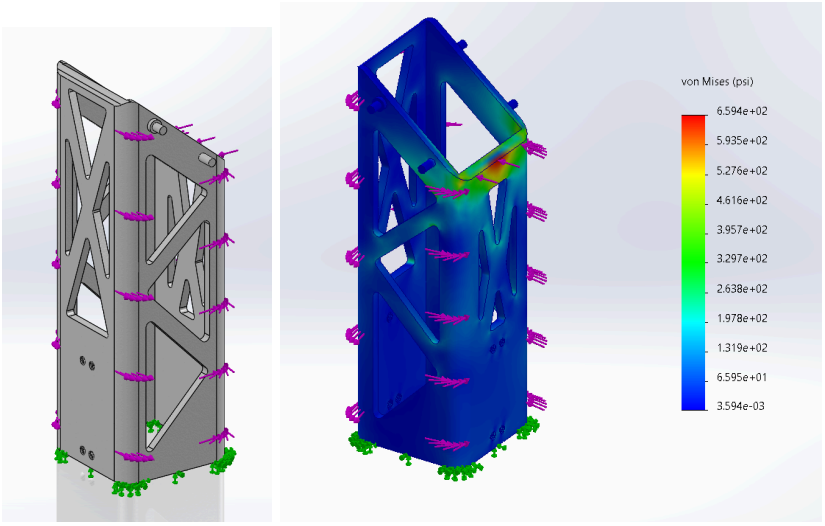

Fig. 24: Optimized calf and second load case FEA

The quad underwent similar optimization and testing with higher load cases because the quad is often horizontal to the body when walking, creating greater bending stress on the component. The first load case was a simple compression load case with 60 pounds of force being applied to the point of connection (Fig. 25). This load case was three orders of magnitude from the yield stress. For the second load test, the load was applied as if the quad was experiencing a step-up motion from the ladder. There were 50 pounds of force applied to the bottom connection point, and the hip mount point was restrained (Fig. 26). This test also experienced far less stress than ABS's yield strength. It is important to note for all of the FEA tests conducted, these are ideal loading conditions for a robot whose kinematic movements are being estimated. While the numbers are very promising right now, these are ballpark estimates being used to inform the design choices we make while engineering components. For further testing, we will create a full-scale leg prototype that will be used to test basic kinematic movements and we will perform tests to determine a baseline of allowable stress before failure.

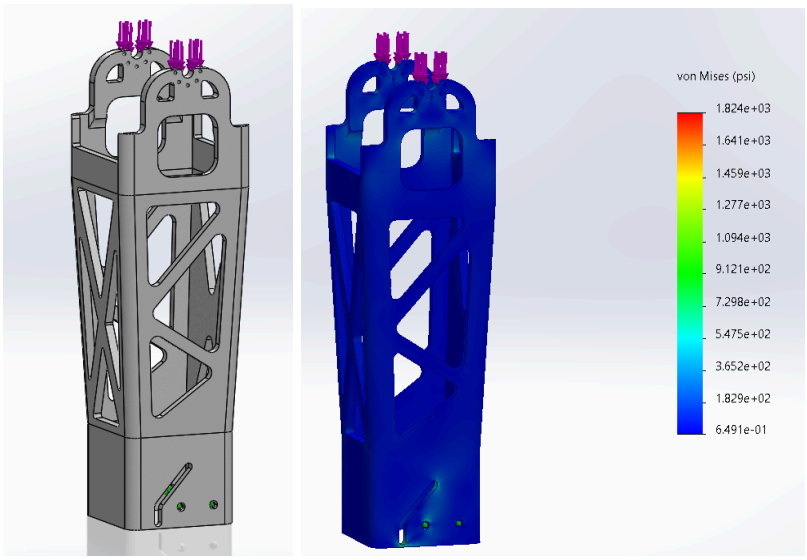

Fig. 25: Quad FEA load case 1

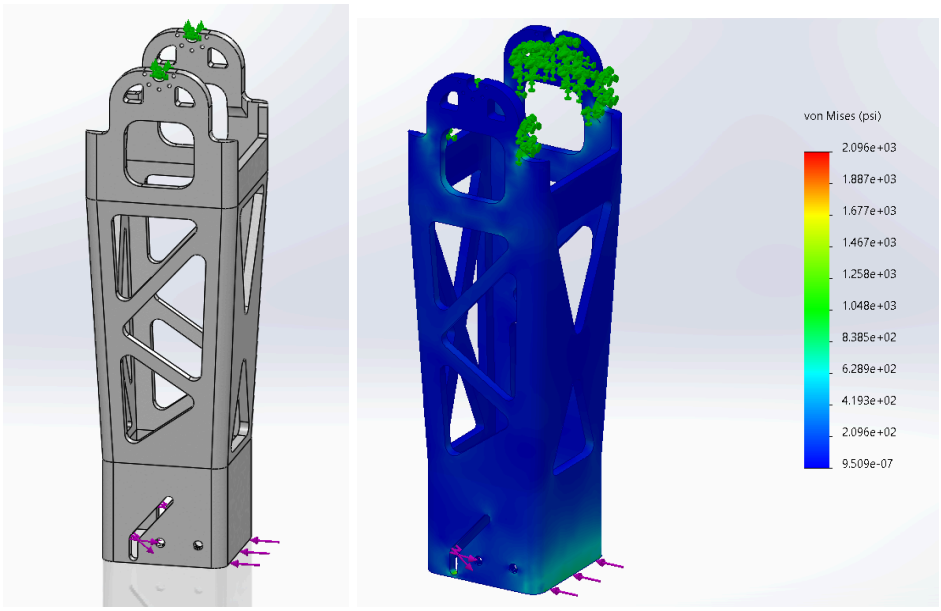

Fig. 26: Quad FEA load case 2

The process of designing the arms was similar to the legs. While there was no “knee” to design around, the arms had the challenge of including three degrees of freedom in the shoulder. The final design for the arm weighs 2.5 pounds, with a total length of 27 inches measured from the shoulder. This roughly resembles the dimensions of the average man. The arms were

designed to be lightweight for efficient movement and to reduce stress on the motors. To enable this, the elbow joints have 1 degree of freedom to enable upward and downward mobility. The shoulder brackets (the parts connected to the shoulder motor) have 2 degrees of freedom, allowing the entire arm to rotate around its central axis and move laterally in and out from the torso. The parts for the arm were created independently. The forearm and bicep were designed to be simple and lightweight to adhere to the robot's weight restriction of 33 lbs. After a simple initial design was created, FEA analysis was conducted to identify modes of failure and further optimize the design. A torque load of 10.6Nm, the maximum torque exerted by the motor, was applied at the elbow joints. Originally, lots of stress was prevalent around the brackets of the elbow (Fig. 27). To mitigate this, we decided to replace the ABS bracket with aluminum so that this piece is more resistant to torque. Moreover, cuts were made in parts of the arm that had insignificant amounts of stress, reducing the overall weight.

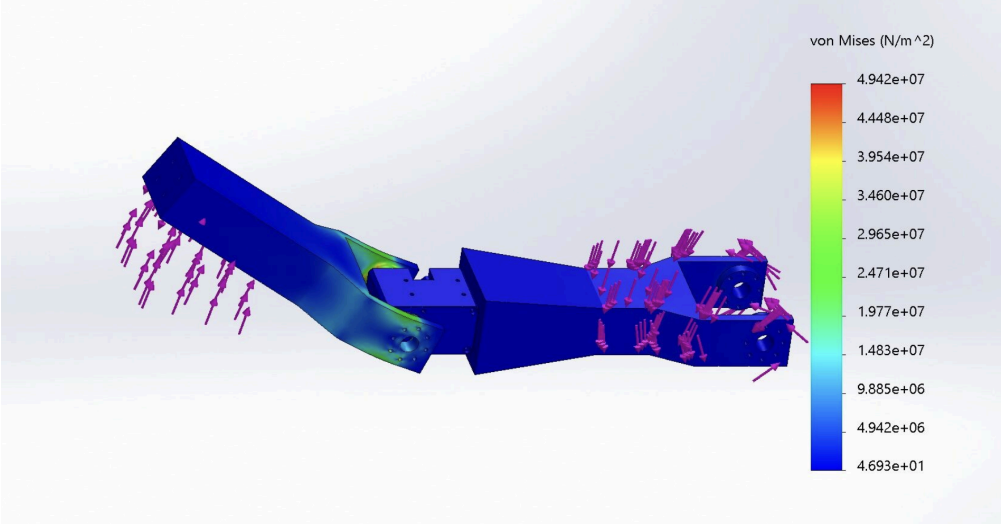

Fig. 27: Original unoptimized arm assembly

After the aluminum bracket was added and the design was optimized, we ran a second test of FEA to ensure the design was feasible (Fig. 28). The design was optimized to resemble a

generic truss structure to create ease of manufacturing. While we intend to 3D print the arms, if necessary, the slender nature and simplified optimization give us the ability to use standard stock ABS blocks with a water jet to create the arm components. Each of the components was also tested individually. The forearm and bicep were tested with a 15 lb axial load and 10 lb shear load applied at the ends of the parts. This loading was chosen to approximate the portion of the weight of the robot borne by the arms when in the four-wheeled configuration. The forearm was found to have roughly 10 times less stress than the yield strength of ABS (Fig. 29). The bicep performed much better under the same loading conditions, with the majority of the part experiencing minimal stress (Fig. 30). The highest stress occurred at the screw holes in both parts, with relatively low stress on the rest of the part. Therefore, these attachment points should be made of aluminum, allowing for higher loads on the arm. Alternatively, increasing the thickness of the attachment points could improve these stress concentrations. Further testing, such as kinematic and allowable stress before failure, will be conducted on a full-scale prototype to further improve the design and functionality of the arm.

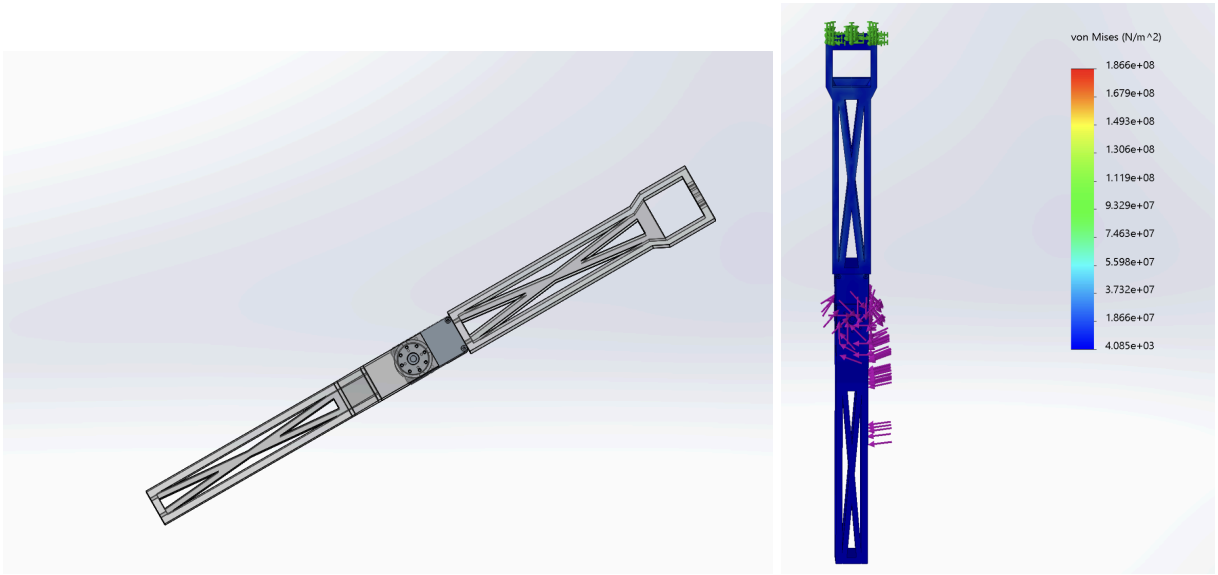

Fig. 28: Final Optimized Arm

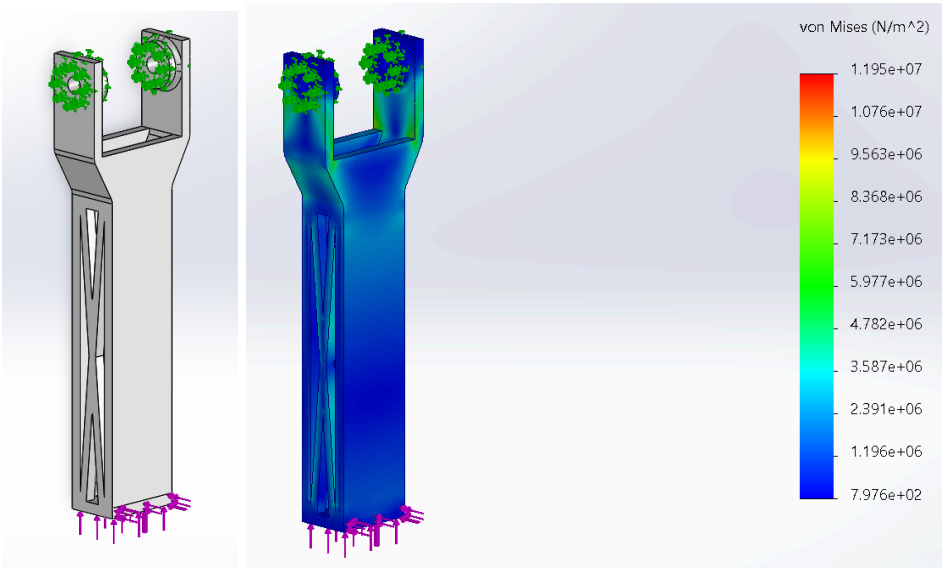

Fig 29: Forearm with 15 lb Axial Load and 10 lb Shear Load

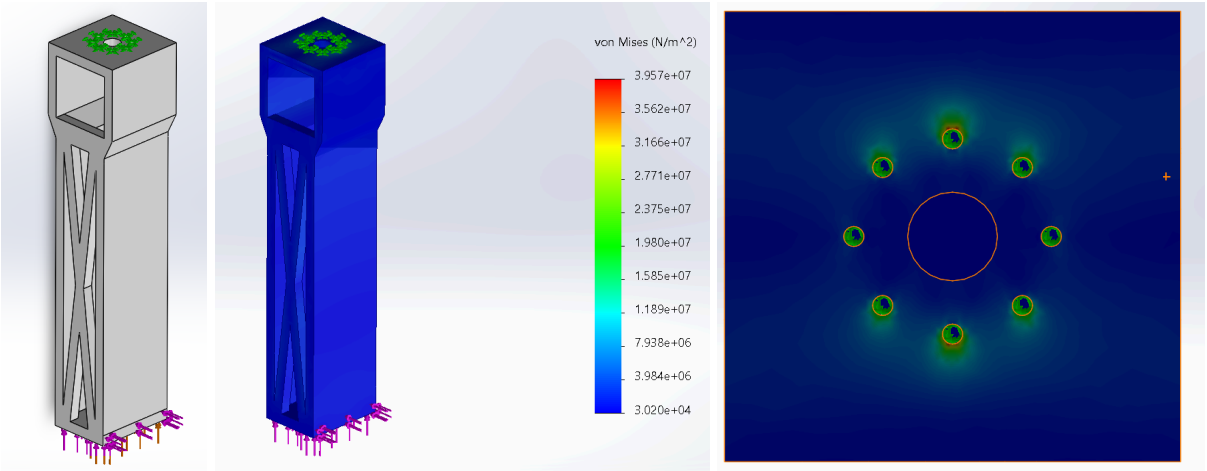

Fig 30: Bicep with 15 lb Axial Load and 10 lb Shear Load

The torso design is trapezoid-shaped with a maximum width of 13.5 inches, a minimum width of 8 inches, a height of 12 inches, and a depth of 5 inches. The design is hollow inside

with a wall thickness of 0.5 inches and has been optimized with FEA. The original torso design has already been discussed in some detail, but the original design was found to be much too bulky and large. The design was reduced from a maximum width of 20 inches to a maximum width of 13.5 inches. This decision was made due to the suggestions from our advisor and an early topology optimization that was performed with basic loading scenarios (Fig. 31). The topology optimization revealed that we could severely cut the size and fullness of the sidewalls on the torso to reduce the final total weight.

The total weight of just the torso is 5.7 pounds and is still the heaviest single component on the robot. Despite the optimization, the reason this component still needs to be so bulky is that the size of the robot makes the torso naturally large, and the wall thickness of 0.500 inches is required to provide rigidity to protect the electronics that will be stored inside. Additionally, there is a 0.550-inch diameter vertical rod that runs through the torso, connecting at the bottom to a horizontal bar that serves as the connection to the hips, allowing the torso to rotate relative to the hips. The motors are mounted to the bottom of this bar with brackets and connected to the quad. This rod is used to allow the robot to rotate freely and point important censors in the direction of information. It also allows the robot to pick up and move components in its workspace without having to navigate extensively.

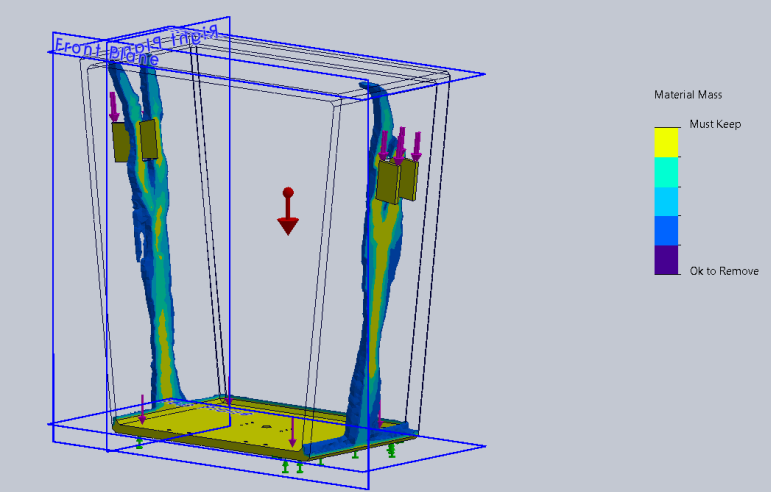

Fig. 31: Early torso topology optimization

Once the final design of the torso was created, the design was tested with FEA to check if the shoulder mounts could distribute the load from the shoulders effectively (Fig. 32). With 20 pounds of force applied to the center of the torso and each shoulder, the torso experienced several orders of magnitudes of less stress than ABS can handle. This is encouraging because although the robot will be carrying things in the torso, the weight of the electronics will not exceed 5 or so pounds, allowing the torso to operate in conditions more favorable than the ones tested. Additionally, the shoulders will likely not experience more force than 20 pounds unless the robot falls, is quickly transitioning to quadrupedal mode, or lifting something heavy.

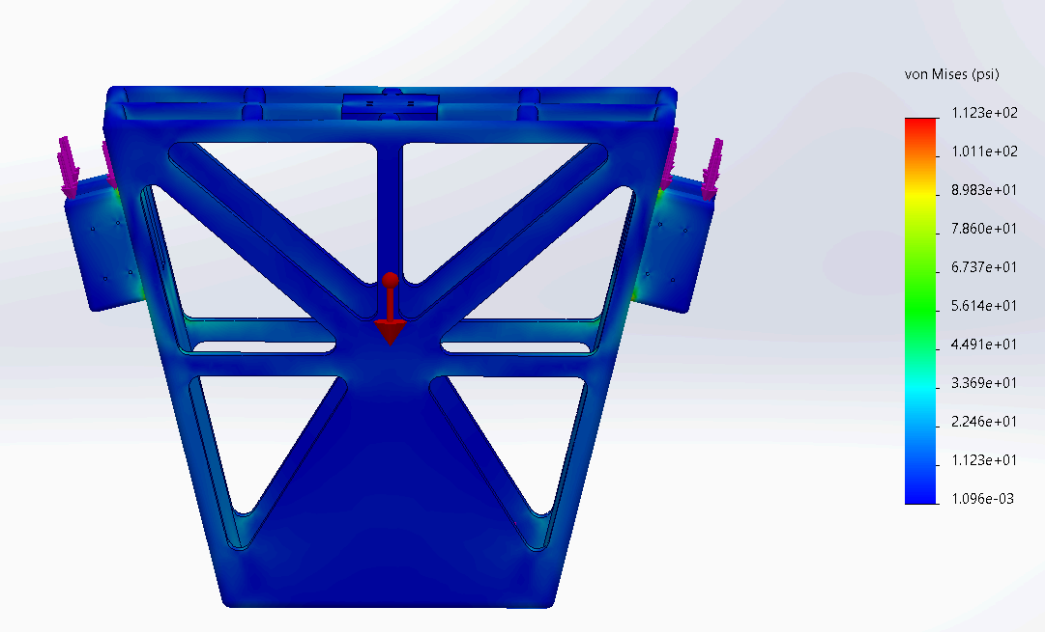

Fig. 32: Optimized torso FEA

As mentioned while discussing the degrees of freedom, the torso only has one degree of freedom despite originally planning to be able to lead forward. The reason this degree of freedom was eliminated was because the degree of freedom posed a threat to the balance of the robot and offered very little in return. The legs can achieve a little bend without creating the worry of instability. By adding a degree of freedom in the torso that would allow the robot to bend forward, we would have been creating another potential point of failure and a structural instability that would have potentially compromised the robot's ability to stand upright.

Moving forward with the design of the torso, we need to determine the best way to print and assemble it. The large component means it needs to be printed across multiple sessions using multiple printers. This means dividing the torso into regions of print with cracks that can be attached to assemble the full torso. This does not pose as large of a problem as it does with the other components, however, because the torso experiences a rather insignificant loading case, and it has thick side walls.

Design Refinement

After testing the initial design, several changes had to be made before the prototyping stage. Although the FEA demonstrated that the designed models would be able to bear the intended loads, the designs needed to be altered. Mainly, the knee connections, hip design, and shoulder design needed to be updated to ensure the robot could be appropriately manufactured and assembled. Additionally, the manufacturing processes and infill values of 3D printed parts needed to be tested in order to balance manufacturability and component strength.

The first element of the design refinement stage was changing the knee connection components. Originally, the knee was designed to have a spring-damper system that acted as a passive support rod that allowed the leg to bend as the motors in the knee bent the leg. The system was designed to emulate a hamstring muscle and to reduce the passive power consumption required to keep the robot upright while in a standing or bent-over position. After being designed, the spring system was manufactured and assembled on a single leg. While the spring system functioned in an upright position, the final assembly could not consistently remain intact while being run through a general bending motion (Figure 33). The main identifiable reason for this was the method of assembly that did not allow for a tight enough connection to hold components together while they experienced uneven stress while bending.

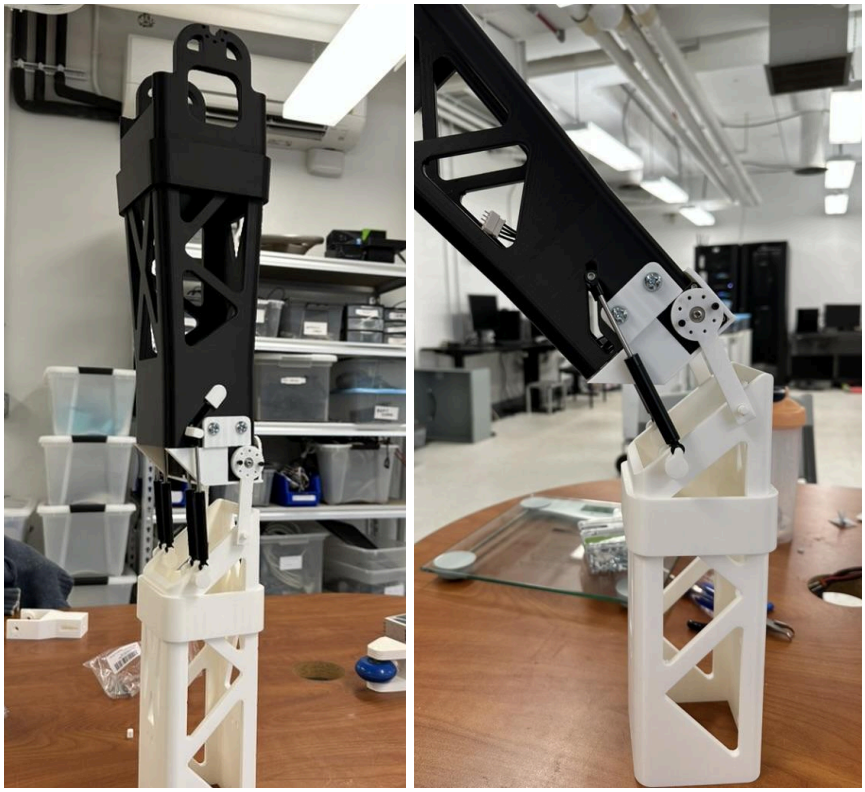

Fig. 33: Image of a passive and half-bent leg with the damping system

The result of identifying this design deficiency was the redesign of the knee connection component. Originally, it was a major concern that the PLA would not be durable enough to withstand bending and rotating forces, but the switch to ABS granted increased flexibility that gave us confidence in a simplified redesign. Upon redesigning the part, the component was attached to the same original connection points on the calf to maintain the same range of motion. The profile, however, was designed so that the force was borne by a triangular profile and placed at the closest point to the mounting pegs (to reduce bending stress). After a few iterations of manufacturing to align the holes and optimize the triangular shape, the final knee-to-calf connection component was installed on the robot (Figure 34).

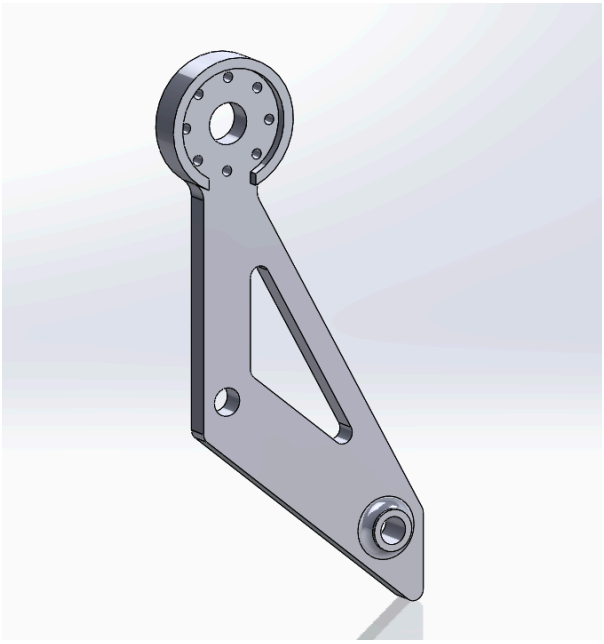

Fig. 34: New calf to knee connection bracket

The second major element of our design refinement was to redesign the hip component. There were several major difficulties that led to a required redesign of the hips. The first, which was a concern with every large component, was the need to split large prints into multiple pieces. The hips were originally 24 inches wide, which we figured would create an increased leg base and increase the stability (Figure 35). This presumption, however, was ill-founded. The wide base made maneuvering the robot difficult and increased the moment arm to the central mounting point. This meant that as the legs bore more weight, the bending stress the hips experienced was increased, ultimately leading to a fatigue-related failure.

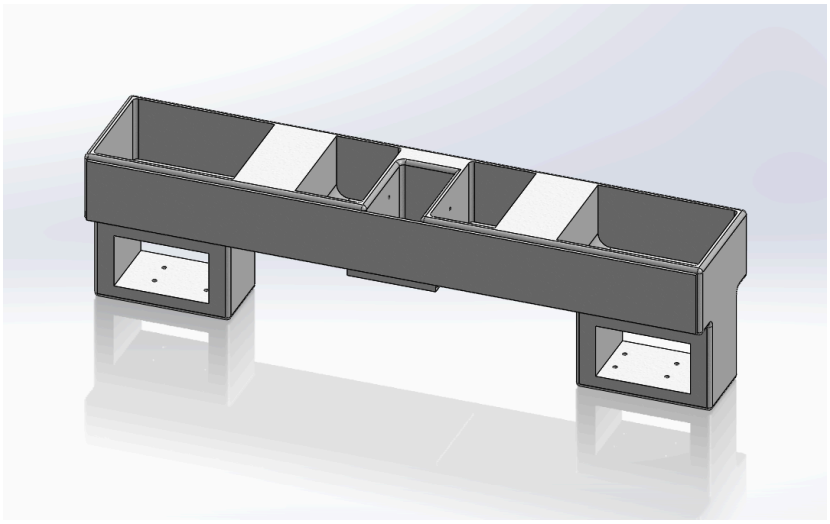

Fig. 35: Intermediate hip design without added support or width

The redesigned hips had a few key changes that increased their strength. The first of these changes was the reduction in their width. They were shortened from the original 20 inches to 15 inches. This reduction led to a moment reduction of roughly 100 in-lbs at the central mounting point. Another change was the increase in wall thickness and a slight shape redesign. The walls were increased in width in order to increase the cross-sectional area and moment of inertia. The final major change was an increase in the gap in the hip motor mount slot. When working with ABS, we often experienced shrinking or warping of certain features due to the cooling complexity associated with ABS. This meant that while our components were designed with some tolerance in mind, the warping caused a change greater than that tolerance. This led to motors experiencing a press fit instead of a loose fit that was originally intended. By making these changes, the hips became more functional, durable, and were better suited for the environment specified in the original contract.

The shoulder component experienced troubles similar to hips. Mainly, the use of ABS resulted in warping that created a fit that was too tight for the motors to be removed after insertion. This was fixed, so an increased tolerance was added. Another problem was the wiring

access within the component. The wiring channels had to be relocated to increase the ease of installation and decrease the stress on the wires (Figure 36). Finally, additional mounting brackets needed to be ordered so there would be a sufficient connection of the arm to the shoulder motor.

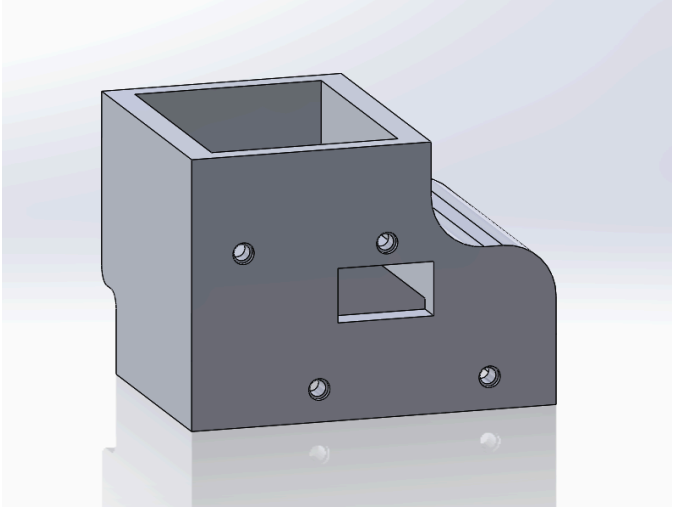

Fig. 36: Finalized shoulder component

By changing these identified elements and components of our design, we could continue into the prototyping and testing stage, where we could observe how whole systems interacted with each other. Although certain elements had been printed and "prototyped" before the official prototype stage, a key element differentiating these examples would be the actual installation of motors and the preliminary testing to ensure desired functionality.

Prototyping and Testing

The prototyping stage was the most iterative part of the entire design process. One major challenge throughout the prototyping stage was getting the motors to function in a coordinated

manner. The actual code structure will be discussed below, but the syncing of motors was an issue that presented the need to iterate the design frequently. Because of the estimated weight of the robot, the knees and hips were designed to use two motors acting in parallel. These parallel motors, although sufficiently strong to bear the weight of the robot, were incredibly difficult to sync. This failure in syncing led to many components experiencing moments about their central axes while testing, resulting in the occasional fracturing of the component.

During the prototyping stage, we also changed minor details with each reprinted version of a part. We started with a bottom-up approach, focusing on the legs first. This was reasoned because the legs would experience the most stress while under regular load cases. They were also seen as the most complex system, so the most time was dedicated to getting them to work. Some small changes that were made include increasing wall thickness, creating calf mounting points, changing side cutout geometries and locations, and tweaking infill percentages. A constant struggle throughout this project was balancing the infill percentage with the manufacturability and weight. While increasing the infill made components much stronger, it also increased the amount of material and time needed to manufacture a single part. Additionally, it increased the weight of the robot. By variably adjusting the infill percentage, we hoped to achieve a level that could be impact-resistant and strong, but lightweight and manufacturable. Because of strength requirements in the legs, leg components were often manufactured with higher infill percentages than other components. They also support increased weight from the foot mechanisms designed by our advisor.

The arms were much easier to work with than the legs. Although there was a 3-degree-of-freedom motor cluster in the shoulder, the lack of parallel motors meant that syncing did not result in any fractures or damage to components. The one difficulty of prototyping the

arms, however, was the manufacturability aspect. The arm components are not as large as the leg components, so they did not need to be split into separate prints, but they were very thin and narrow. This meant that when trying to attach motors axially, the working space was tight and often resulted in improper connections. Additionally, there was an incident during the prototyping stage where the arm assembly fell off a workstation and broke the bicep component. Despite this setback, it taught us where the weak point in the bicep was, and changes were made to the final design.

The final element of the prototyping phase was assembling subassemblies and finding a place to mount the robot. Although not our first choice, to connect components that had to be separated during printing due to size restrictions of the printing bed, we used Loctite plastic adhesive. This choice was made largely due to weight restrictions and time restraints. By adding collars with screws and bolts, additional weight would be added that we could not afford to add. Adding collars and screws increased the complexity of the design while only creating stability at points instead of along the entire seam. The Loctite solution allowed our team to apply the adhesive and wait for it to cure and then receive a level of strength that was greater than the yield stress of the 3D printed ABS component.

Coding Infrastructure and Programming

The humanoid robot was programmed using ROS (Robotic Operating System) and C++. This enables the mobility of the robot via a remote control. We decided to use ROS because it provides a flexible and well-supported framework for developing robotic systems. ROS allows for the software to be more modularized using special components called nodes. Each node can either send or receive information to other nodes. This modularity ensures real-time

communication and scalable infrastructure. Another major benefit of ROS is its wide range of open-source packages. This facilitates the motor and remote control connections.

Why C++

We chose C++ as the main programming language because of its low speed and compatibility with hardware interfaces. Since the robot communicates directly with the motors and needs to process real-time feedback, performance and efficiency were important. The language gives us more control over memory usage and timing, which are crucial in mitigating any delays. C++ also integrates well within the ROS ecosystem and the Dynamixel Software Deployment Kit (SDK). The extensive documentation of the Dynamixel SDK in C++ provided a framework for integrating our software to allow motor control.

Architecture Design

We designed the software architecture of the robot to ensure scalability and real-time performance. All metadata from the controller is published and centralized to ensure a single point of access. Each limb is organized into clusters, which contain a set of motors. These clusters subscribe to unique segments of the shared data source, which are then communicated to the motors for execution

Motor Communication

To control each motor, we use the Dynamixel SDK to provide direct low-level access to the motor's internal registers. The communication is handled over a serial USB port using the packet protocol version 2.0. Through this interface, we can send precise instructions to each motor and

receive real-time feedback. Common operations include writing data to configure the motor's behavior, such as setting target positions, and reading data to retrieve the motor's current position. These read/write operations are performed via specific register addresses defined in the Dynamixel SDK documentation.

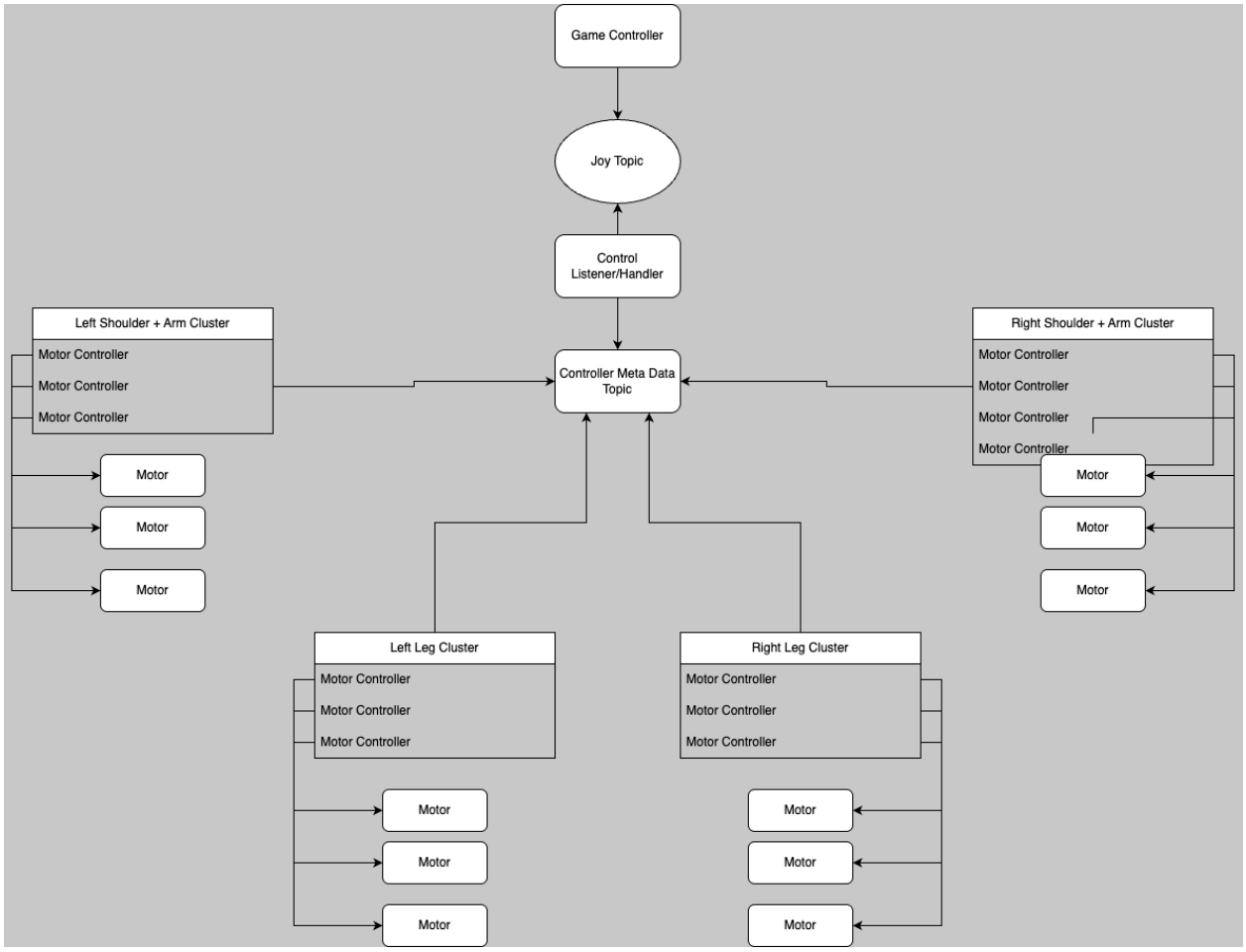

Fig. 37: General coding architecture

```cpp
Motor_Controller::Motor_Controller(ros::NodeHandle &nh, int motor_id, int baude_rate, int starting_position, int max_degrees, bool reverse_position = false)
{
    protocol_version = 2.0;
    port_handler = dynamixel::PortHandler::getPortHandler("/dev/ttyUSB0");
    packet_handler = dynamixel::PacketHandler::getPacketHandler(protocol_version);

    this->motor_id = motor_id;
    this->baude_rate = baude_rate;
    this->reverse_position = reverse_position;

    publisher = nh.advertise<std_msgs::Int32>("/motor_controller_" + std::to_string(motor_id) + "/goal_position", 1);
    motor_connected = this->connect_motor();
    if (!motor_connected)
    {
        return;
    }
    operating_mode = 4;
    drive_mode = reverse_position ? 1 : 0;
    this->set_operating_mode(operating_mode);
    this->set_drive_mode(drive_mode);
    this->starting_position = this->set_starting_position(starting_position);
    this->set_max_motor_degrees(max_degrees);
    this->set_torque(true);
    this->add_offset();
    this->reset_motor();
    ros::spinOnce();
}
```

Fig. 38: Motor establishment function

```cpp
void Motor_Controller::write_goal_position()
{
    uint8_t dxl_error = 0;
    int dxl_comm_result = packet_handler->write4ByteTxRx(port_handler, motor_id, 116, goal_position, &dxl_error);

    if (dxl_comm_result != COMM_SUCCESS)
    {
        ROS_WARN("Error writing goal position of Motor with ID %d: %s", motor_id, packet_handler->getTxRxResult(dxl_comm_result));
    }
}
```

Fig. 39: Motor movement function

```cpp
int Motor_Controller::get_present_position()
{
    uint8_t dxl_error = 0;
    int32_t position = 0;

    int dxl_comm_result = packet_handler->read4ByteTxRx(port_handler, motor_id, 132, (uint32_t *)&position, &dxl_error);

    if (dxl_comm_result != COMM_SUCCESS)
    {
        ROS_WARN("Error reading present position of Motor with ID %d: %s", motor_id, packet_handler->getTxRxResult(dxl_comm_result));
        return present_position;
    }

    present_position = position;
    return present_position;
}
```

Fig. 40: Current motor position function

Sync and Motor Homing Issues

During testing, we encountered several challenges related to syncing and motor homing. Our goal was to have each motor align to a default “zero” position that corresponded to the desired neutral posture of the robot’s limbs. One issue was using multiple motors in parallel, particularly in the hips and knees, to support the robot’s weight. These motors often failed to remain synchronized, which resulted in imbalanced motion and unexpected forces on components. Differing positions and torques between motors in the same joint caused torsion around the joint, risking damage to components. Another issue was motor homing. Due to mechanical offsets during assembly, a motor set to 0 degrees did not always correspond to the correct physical alignment. This offset made it difficult to ensure symmetry and consistency through mirrored parts. Furthermore, without an absolute reference, even small errors could accumulate over time and cause unpredictable behaviour. These challenges highlighted the need for a reliable zeroing calibration process, which was done by manually setting each limb to its natural default position, then calculating the number of degrees moved by the motor and subtracting this number from the original value. Additionally, the motors experienced issues related to negative position values, leading to a sudden and violent repositioning on robot startup. This issue necessitated additional code to ensure the correct starting position of each motor when the robot starts. All of this motor calibration was done through Dynamixel Wizard.

Final Robot Design

The final robot design was the culmination of a year’s worth of work. While not entirely dissimilar from the original mockup proportions or shape, the final robot is significantly improved in design and verified by component testing. Although not all of the project’s original

goals were achieved throughout the course of this working year, a serious and significant step has been made from where we began toward the final project's goals.

As we began finalizing the robot and polishing the final design, we wanted to define our testing goals. Originally, we set out to have the robot fully functional with the ability to walk and roll. Along the way, we experienced several delays and setbacks that made these goals unrealizable. We refined our test goals to have operational arms and rotatable, and inflatable wheels. We ended up meeting this goal and achieving an end state that we were proud of. The final robot (Figure 41) was even capable of forming the 'UVA' arm symbols often seen at sporting events.

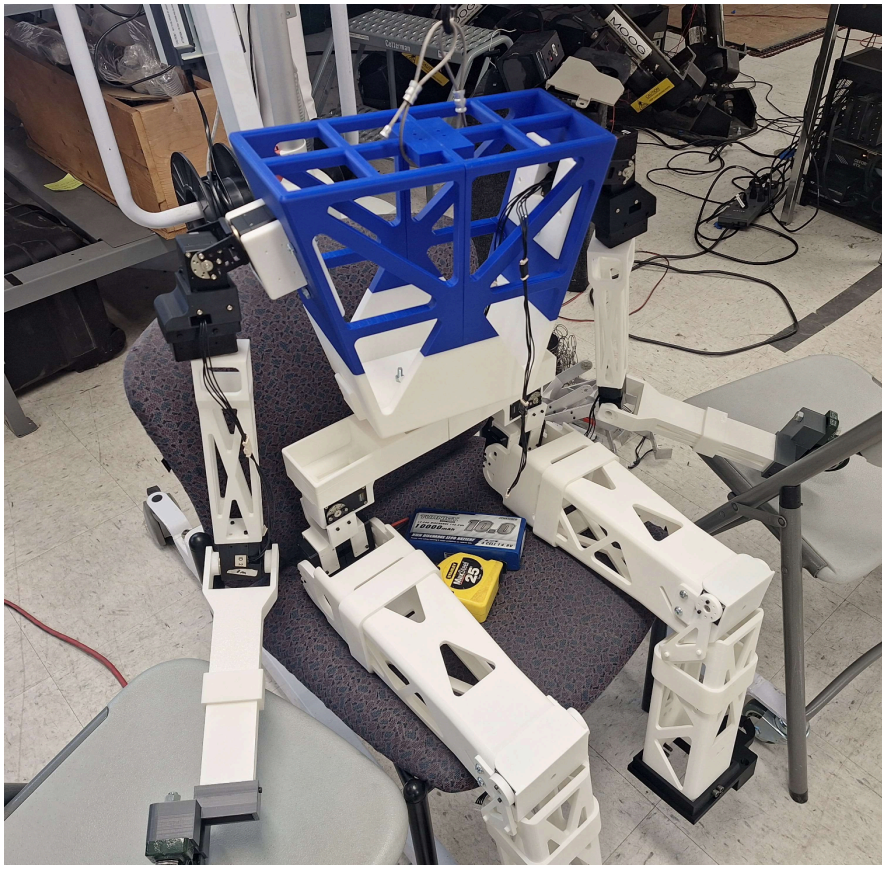

Fig. 41: Final seated robot unwired

A portion of the semester was spent planning the electronics placement on the robot. The wiring for the wheels was attached to the back of the hips to prevent any dragging along the ground (Figure 42). The robot also had an onboard series of pumps and valves that inflated the wheels. The wheels were designed so that when they were not inflated, the rubber exterior was pulled taught around the inner shape that was flat on two sides. This allowed the wheel to act as a foot when not inflated and transform into a wheel for rolling when inflated. This design is an applied version of what can be seen in Figure 9.

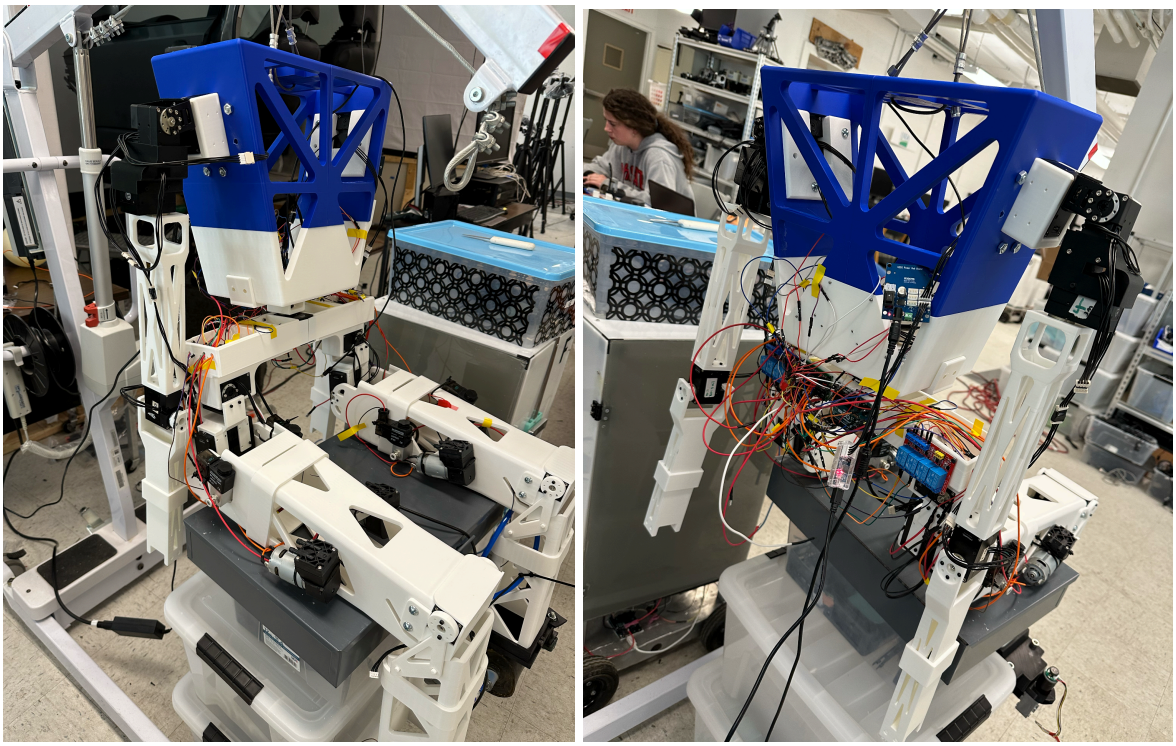

Fig. 42: Final wiring installed on the robot

Because we were unable to achieve everything we wanted to this year, our group has a list of things we believe could be improved on to get the final product even closer to the final desired end state. These topics vary from changes to our design we believe would improve it to areas and tasks to focus on when granted additional time to work.

Future Work

While we were not able to achieve all the goals we set out to at the beginning of the semester, we were still able to get a deeper understanding of the design process and successfully created a lightweight robot frame using 3D printing. With more time, money, and a larger 3D printer, we likely could have greatly improved on our design through multiple iterations.

One of the main sources of weight on our robot came from the Dynamixel motors that were used. The robot's frame and the motors together were a total of 21.6 lbs, with 13.6 lbs accounting for the motors alone. The robot used a total of 19 motors, which were 0.72 lbs each. They are also rather large motors, and they made it difficult to incorporate them into the design. They also had a hard time syncing with each other and moving at the same time. The knee joint was designed with two motors to lift the calf and hold the weight of the robot, and during testing, the two motors had extreme difficulty moving at the exact same time as they were programmed. This resulted in the light-weight knee components snapping repeatedly and needing to be replaced. The motors also do not encode. This is a device mounted onto a motor shaft that uses rotational motion in order to monitor the speed, position, and direction of the motor. This is an extremely important feature when you need precise motor movement, as the robot does. Instead, the Dynamixel motors keep track of their position based on the inputs to the motor, leading to small offsets from the true position that accumulate over time. The main goal with new motors would be to find ones with a higher torque-to-weight ratio, which will help decrease the weight added to the robot while still ensuring the motors have enough torque to move the components and hold up the weight of the robot. This could be done through the purchase of a new type of servo motor or by designing a gearbox that would mechanically increase the torque of the motor

and therefore the load that can be placed on the motor. A potential new motor that could be used is a DC brushless motor, which has extremely high efficiency and a compact and lightweight design that has a high torque output, making them ideal for mobile robots. They also require low maintenance and have relatively long lifespans, and have precise control that allows you to control the speed and the torque. When used with encoders that have positional feedback, they are extremely useful for coding the movement of the robot.

Additionally, replacing the motors in the two-motor joints with single larger motors would be beneficial. This would remove the synchronization issues in the two-motor joints and also simplify the construction of these joints, allowing for a more compact design. While the single motor would be larger than the two motor setup, it is likely that removing the duplicate supports, attachment points, and electrical components would both reduce the total weight as well as decrease the complexity of these areas of the robot and simplify the motion of these joints. Using encoders would reduce the synchronization issues in these joints; however, it is likely to persist to some degree unless a single motor setup is adopted.

The wiring of the final robot can also be improved. The final wiring was an amalgamation of different types and colors of wire. Run from the back of the hips, the wiring job could be improved by soldering wires of calculated length to components instead of using long strands of daisy-chained wires. The onboard electronics could also be modified to reduce the total number of wires needed to be run through the robot. While including mechanical relays makes the logical processes simple, it significantly increases the wiring complexity onboard the robot. By instead using smartpin microcontrollers with access to higher voltage capabilities, such as the Arduino Uno, which can use 12V, we could eliminate the need for physical relays that require a large amount of wire. Another key aspect of the wiring that needs to be modified is the

electronics' locations on the robot chassis. While the back of the hips is an acceptable location for the time being (due to the robot's limited mobility), the final location needs to be padded or compartmentalized so bumps or falls will not interfere with their function. This could be most easily achieved by using the central torso compartment more efficiently or other portions of the hollow components. Finally, another aspect of the wiring that needs to be fixed is the impromptu and uncommunicated locations of holes. While it may be convenient to drill a hole wherever needed, the removal of material from certain places on the robot results in the inherent weakening of the structure. To reduce the weight of the robot, we are required to operate at a much lower factor of safety, meaning that these components cannot experience much more than the designed maximum loads without breaking. By removing the material, it increases the variability and unknowns associated with these maximum allowed loads.

The final physical change that needs to be made to the robot is the reduction of weight from the final design. The intention of using 3D printed ABS was to reduce the total weight of the robot, but by adding heavy pneumatic equipment, it neutralizes any of the benefits of using ABS. We estimated that roughly 23 pounds of pneumatic-related components were added to the robot to accommodate the wheels. If we used pneumatics instead of traditional servo motors for the legs and arms, we would be able to accommodate this weight. Instead, however, we have added an insurmountable amount of weight to the robot so it can no longer walk as intended. Because of the weight increase as a result of the pneumatics, it is recommended that if there is onboard pneumatics for the feet, there should also be pneumatics for the arms and legs. Pneumatics would increase the strength of the legs and arms past what is achievable on a relatively similar weight servo motor.

Apart from the physical changes that need to be made to future versions of our robot, there are next steps that should be taken to improve the capabilities of our robot. The first subject is finishing and polishing the algorithms for walking and rolling. While the motors create the capability for these motions, the code to make it happen needs to be written. This means developing complex matrices for referential position data that we could use to always know where components are when motors are moved. Additionally, there needs to be an element of feedback that can help the robot communicate with its surroundings. Using electronics like a PID controller paired with an IMU. These devices will give the robot the ability to sense where it is positionally, check if it is level, and make smooth adjustments by increasing or decreasing motor function to achieve levels of balance.

While this short list is bound to expand and change as the project receives more attention and work, it serves as a great jumping off point for the future. Our work this year has made great improvements to the design given to us, and by improving upon these identified weaknesses and goals, we know our design can be improved.

Summary and Conclusions

One of the biggest challenges in robotics today is creating a humanoid robot that can act functionally while still maintaining heightened mobility. There are dozens of companies creating general prototypes and simplistic humanoid robots for commercial use to address these design needs. From Boston Dynamics to Tesla to Ascento and Unitree, each company addresses this design challenge uniquely. Our team, when tasked with creating a humanoid robot capable of completing day-to-day tasks relevant to aircraft carrier maintenance and support, is no different.

In fact, we have drawn inspiration from several of these commercially available models to create our initial design.

While the design objectives we have been given as a team are unique, we have found ways to draw inspiration and combine successful elements from different sources. The two main functions the robot must be able to do are climb a 63-degree ladder and quickly navigate down an aircraft carrier hallway. To have the ability to climb the ladder and for accurate proportions, we looked to the Unitree G1 as a source of inspiration. To have a sense of mobility, we have referenced the successes of the Ascento Pro. Additionally, the Navy, who is the sponsor of our project, has tasked us with creating transforming limbs to achieve the mobile robot they have challenged us to design. This means that the hands and feet must be capable of transforming into wheels and back into their respective traditional appendages. This transformation poses a variety of engineering design challenges, and while the scope of our project was reduced to not include the designing and engineering of these transformable limbs, we are still tasked with designing a frame capable of supporting the transforming kinematics and other movements of the robot.

To achieve this ambitious goal, we started by creating a rough draft of proportions for our robot and focused on motor placement. We then worked with our advisor to devise a plan for the number and locations of the degrees of freedom we would need to be able to support the transforming movements. We also referenced last year's documentation to find out what did and did not work with respect to limb design and motor placement. It was found that the weight of last year's robot was significantly heavier than could be supported, so the number of motors per limb was increased and the weight of each limb was reduced via optimization. We also decided to divert from their design decision to use aluminum for the body and instead opted to use 3D printing to create an ABS frame.

After deciding to use ABS and determining the degrees of freedom, the component design period began. The legs, arms, and torso were designed in a parallel fashion, where the designers could incorporate feedback from the other subteams into their design as each of the designs evolved. The legs were designed to reduce weight while maintaining functional capability. This was mainly seen in the designed range of motion of the leg to bend at a 90-degree angle to climb a steep ladder. This motion required a large range of motion but a strong support. The force of the entire body acting on the leg in bending rather than in compression means that the legs needed to be designed correctly to withstand increased stress. A basic design was created, and using FEA with higher-than-expected load cases, the components of the leg were optimized. This led to a leg design with a total length of 37.6 inches and a weight of 4.8 pounds. The design process for the arm assembly was similar. The arms had rudimentary proportions for their initial draft, and after discussion with our advisor, the total length of the arms was greatly reduced to create better proportions for the final design. Since the arms must be able to rotate to grab the handles of the ladder for support, they must have three degrees of freedom in the shoulders. These degrees of freedom were the focal point for the design process, and the bicep and forearm were created as truss-like structures to maximize the strength of the components while reducing their weight. The bicep and forearm were also optimized through various rounds of FEA to best achieve a good balance of weight and strength. Finally, the torso was designed originally as a large cabinet, but when determined to be unnecessarily large and bulky, the torso was significantly shrunk and optimized with FEA. The hips were also designed to mesh the leg assemblies with the torso assembly, and the shoulders to mesh the arms with the torso.

After designing these components, we proceeded into the second semester of our project, dedicated to the goal of manufacturing the robot. This led to a refinement period where we discovered that while many elements of our design were achievable and very practical, several elements were unrealistic. We began by fixing several issues we identified through the initial manufacturing and testing phases. These changes were mainly the removal of the suspension components in the leg, the changing of tolerances and shapes in the hips, and the redesigning of the shoulder motor mount. We also took time to understand how the motors and systems would begin to interact.

From there, we proceeded into a more formal prototyping and testing stage, where we started implementing larger systems in a manner more similar to what we would expect them to act like on our final robot. We encountered issues with motor syncing and began working out to kinks with coordinating motor movements. We polished and improved our coding infrastructure and developed workarounds for complex motor limitations.

Finally, we moved on to the stage where we assembled the entire robot. We realized along the way that the scope of our project was far too much for us to achieve in the time we had been given, so we reduced the number of things we wanted to make sure were finalized and working before the semester ended. In the end, we managed to get the wheels working and the arms working. We tested each in a manner respective to their designed goals and were met with glaring success. The wheels attached to the feet could spin freely, and the arms could lift up and stay in an upward position. Meeting these two goals demonstrates that our design has a lot of potential, and with some additional work, it could meet all of the design challenge goals.

Despite a year filled with obstacles and uncertainty, our group overcame adversity to produce a final product capable of many of the original design goals. The transition from an

all-aluminum frame to a 3D printed chassis with working inflatable appendages marks a large step toward fulfilling the Navy's contract. Our team went through a rigorous design and selection phase matched with a critical design refinement period to create an end robot capable of moving freely. While there is still a lot to be done, our final design is a large step toward success that we are very proud of.

Appendix A: Bibliography for Research

References

Ascento Robotics. (2024). *Ascento Pro*. Ascento - Secure Assets with Robotics and AI. Retrieved December 12, 2024, from https://www.ascento.ai/

ASIMO. (2024). Wikipedia. Retrieved December 12, 2024, from https://en.wikipedia.org/wiki/ASIMO

Atlas. (2024). Boston Dynamics. Retrieved December 12, 2024, from https://bostondynamics.com/atlas/

Humanoid robot G1_Humanoid Robot Functions_Humanoid Robot Price. (2024). Unitree Robotics. Retrieved December 12, 2024, from https://www.unitree.com/g1

US Navy. (2021, October 20). *Shipboard Autonomous Firefighting Robot (SAFFIR)*. America's Navy. Retrieved December 12, 2024, from https://www.navy.mil/Resources/Fact-Files/Display-FactFiles/Article/2160601/

Appendix B: Detailed Drawings

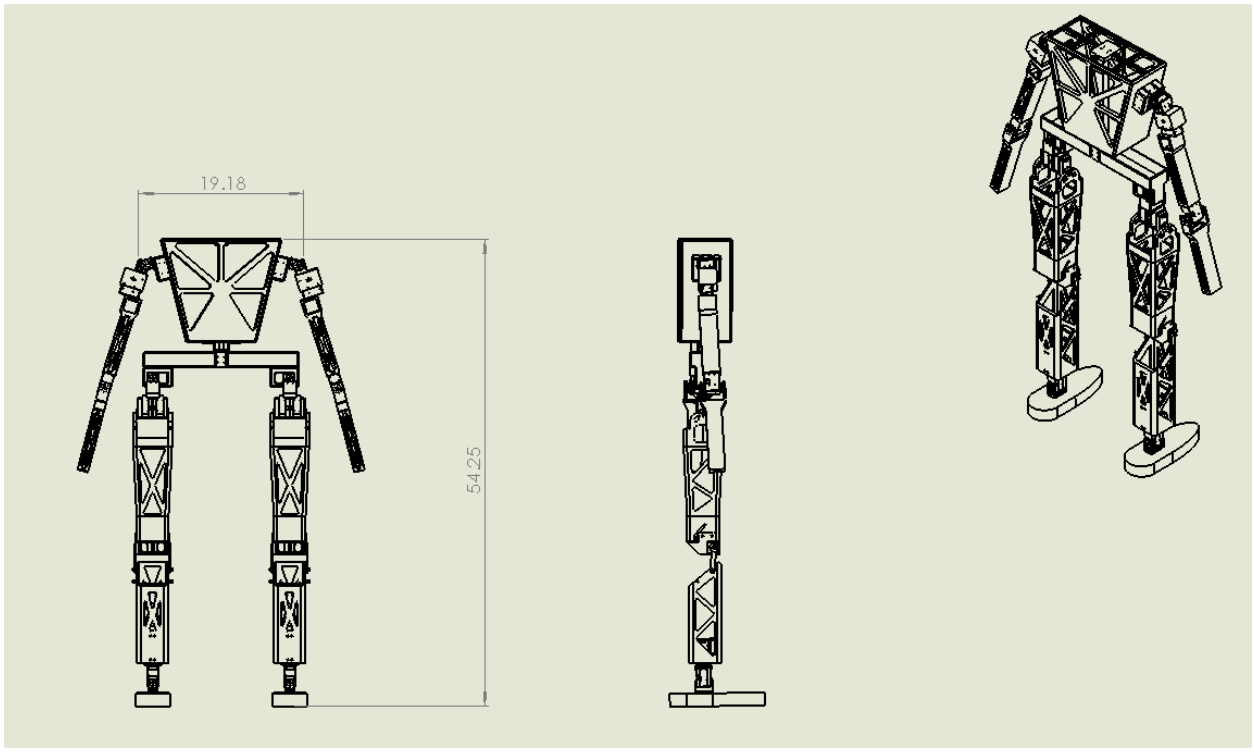

Leg Drawings:

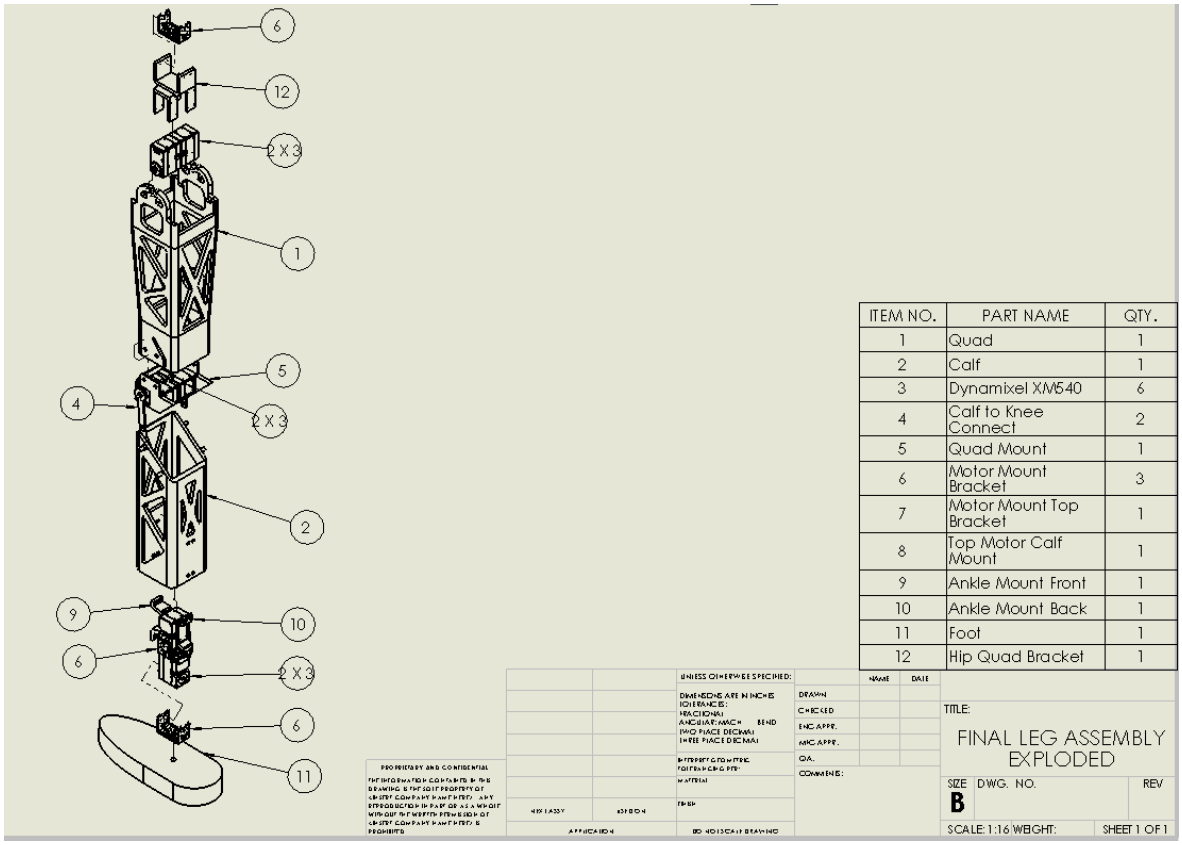

ITEM NO.	PART NAME	QTY.
1	Quad	1
2	Calf	1
3	Dynamixel XM540	6
4	Calf to Knee Connect	2
5	Quad Mount	1
6	Motor Mount Bracket	3
7	Motor Mount Top Bracket	1
8	Top Motor Calf Mount	1
9	Ankle Mount Front	1
10	Ankle Mount Back	1
11	Foot	1
12	Hip Quad Bracket	1

UNLESS OTHERWISE SPECIFIED:
DIMENSIONS ARE IN INCHES
TOLERANCES:
FRACTIONAL
ANGULAR: MACH BEND
TWO PLACE DECIMAL
THREE PLACE DECIMAL
INTERPRET GEOMETRIC TOLERANCING PER:
MATERIAL
FINISH
NEXT ASSY
USED ON
APPLICATION
DO NOT SCALE DRAWING

NAME DATE
DRAWN
CHECKED
ENG APPR.
MFG APPR.
QA
COMMENTS:

TITLE:
FINAL LEG ASSEMBLY EXPLODED

SIZE B
DWG. NO.
REV

SCALE: 1:16 WEIGHT:
SHEET 1 OF 1

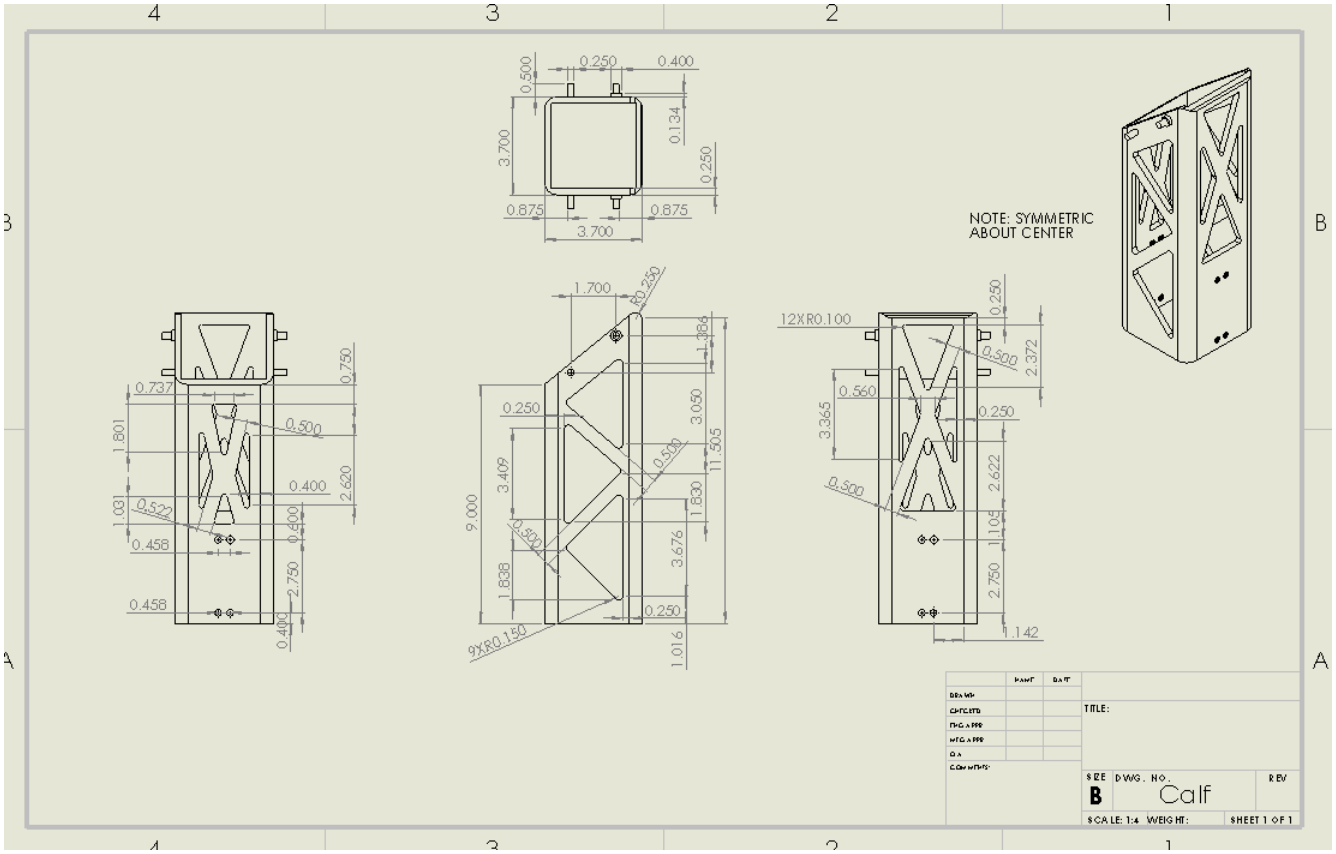
NOTE: SYMMETRIC ABOUT CENTER
12XR0.100
9XR0.150
TITLE:
SIZE B
DWG. NO. Calf
REV
SCALE: 1:4 WEIGHT:
SHEET 1 OF 1

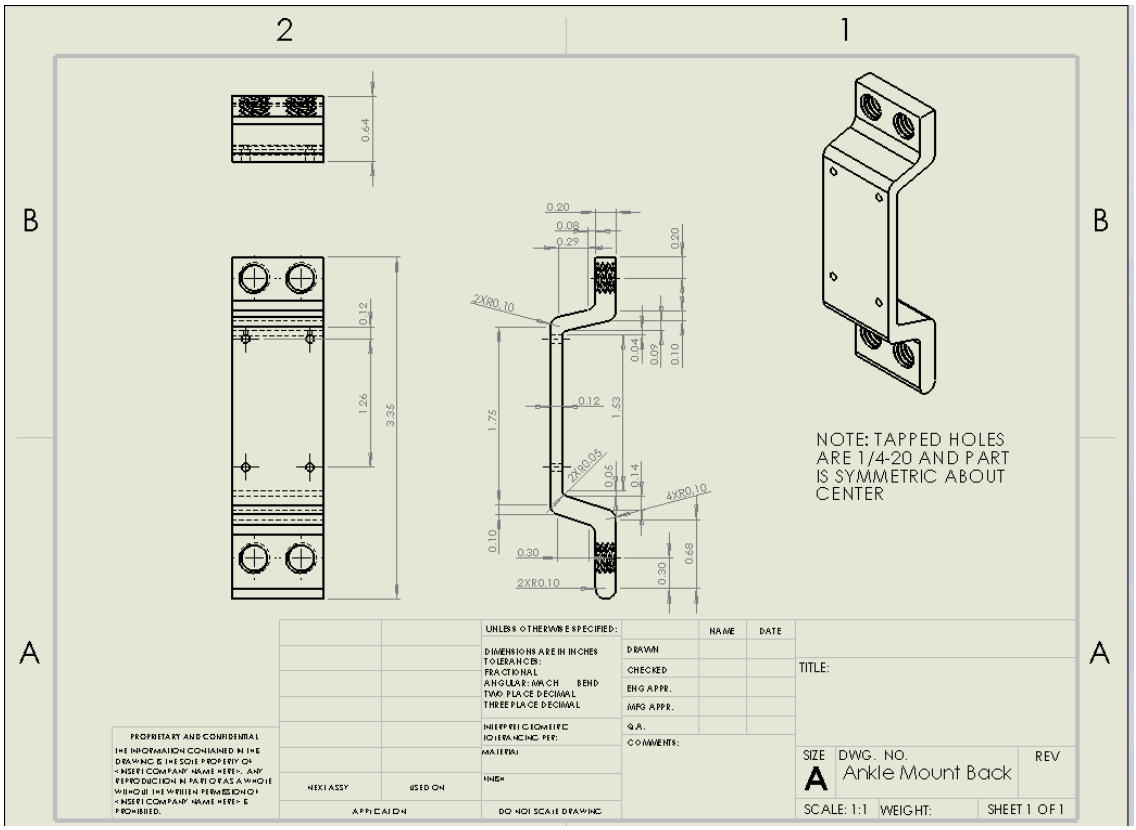
NOTE: TAPPED HOLES ARE 1/4-20 AND PART IS SYMMETRIC ABOUT CENTER
2XR0.10
4XR0.10
2XR0.08
UNLESS OTHERWISE SPECIFIED:
DIMENSIONS ARE IN INCHES
TOLERANCES:
FRACTIONAL
ANGULAR: MACH BEND
TWO PLACE DECIMAL
THREE PLACE DECIMAL
INTERPRET GEOMETRIC TOLERANCING PER:
MATERIAL
NEXT ASSY
USED ON
APPLICATION
DO NOT SCALE DRAWING
NAME
DATE
DRAWN
CHECKED
ENG APPR.
MFG APPR.
Q.A.
COMMENTS:
TITLE:
SIZE A
DWG. NO. Ankle Mount Back
REV
SCALE: 1:1 WEIGHT:
SHEET 1 OF 1
PROPRIETARY AND CONFIDENTIAL
THE INFORMATION CONTAINED IN THIS DRAWING IS THE SOLE PROPERTY OF <INSERT COMPANY NAME HERE>. ANY REPRODUCTION IN PART OR AS A WHOLE WITHOUT THE WRITTEN PERMISSION OF <INSERT COMPANY NAME HERE> IS PROHIBITED.

NOTE: OUTER FILLETS ARE 10mm

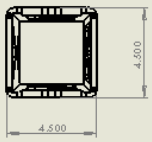

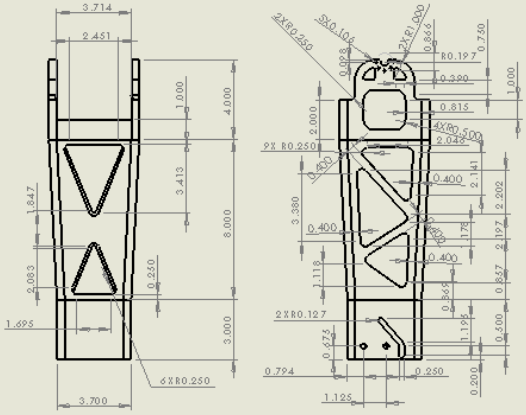

NOTE: SYMMETRIC ABOUT CENTER

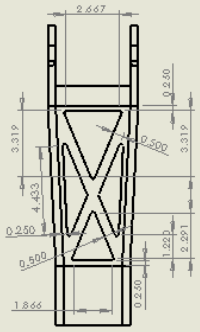

NOTE: ALL WALL THICKNESSES ARE 0.275 INCHES

NOTE: ALL FILLETS ON VIEW ARE R0.100, SYMMETRIC ABOUT CENTER

	NAME	DATE
DRAWN		
CHECKED		
ENG APPR.		
MFG APPR.		
Q.A.		
COMMENTS:		

TITLE:

SIZE	DWG. NO.	REV
A	Quad	
SCALE: 1:8	WEIGHT:	SHEET 1 OF 1

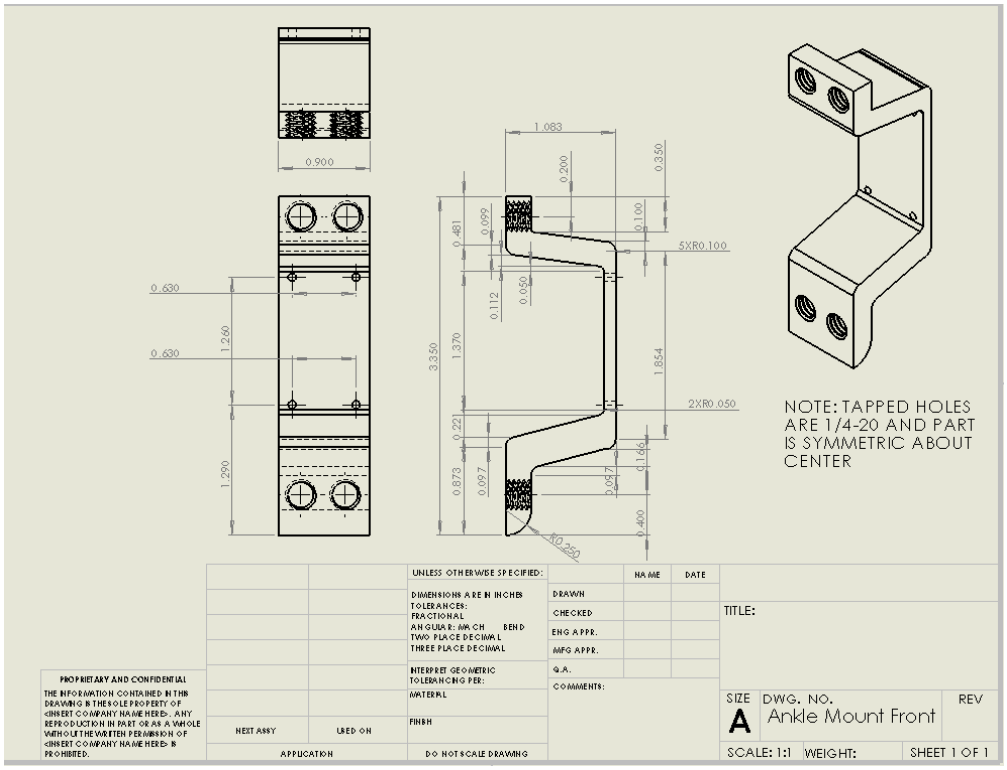
1.083
0.900
0.200
0.350
0.481
0.099
0.100
5XR0.100
0.112
0.050
0.630
0.630
1.260
3.350
1.370
1.854
2XR0.050
0.22
1.065
0.873
0.097
0.097
0.400
1.290
R0.250
NOTE: TAPPED HOLES ARE 1/4-20 AND PART IS SYMMETRIC ABOUT CENTER
UNLESS OTHERWISE SPECIFIED:
DIMENSIONS ARE IN INCHES
TOLERANCES:
FRACTIONAL
ANGULAR: MACH BEND
TWO PLACE DECIMAL
THREE PLACE DECIMAL
INTERPRET GEOMETRIC TOLERANCING PER:
MATERIAL
FINISH
NEXT ASSY
USED ON
APPLICATION
DO NOT SCALE DRAWING
NAME
DATE
DRAWN
CHECKED
ENG APPR.
MFG APPR.
Q.A.
COMMENTS:
TITLE:
PROPRIETARY AND CONFIDENTIAL
THE INFORMATION CONTAINED IN THIS DRAWING IS THE SOLE PROPERTY OF <INSERT COMPANY NAME HERE>. ANY REPRODUCTION IN PART OR AS A WHOLE WITHOUT THE WRITTEN PERMISSION OF <INSERT COMPANY NAME HERE> IS PROHIBITED.
SIZE
A
DWG. NO.
Ankle Mount Front
REV
SCALE: 1:1
WEIGHT:
SHEET 1 OF 1

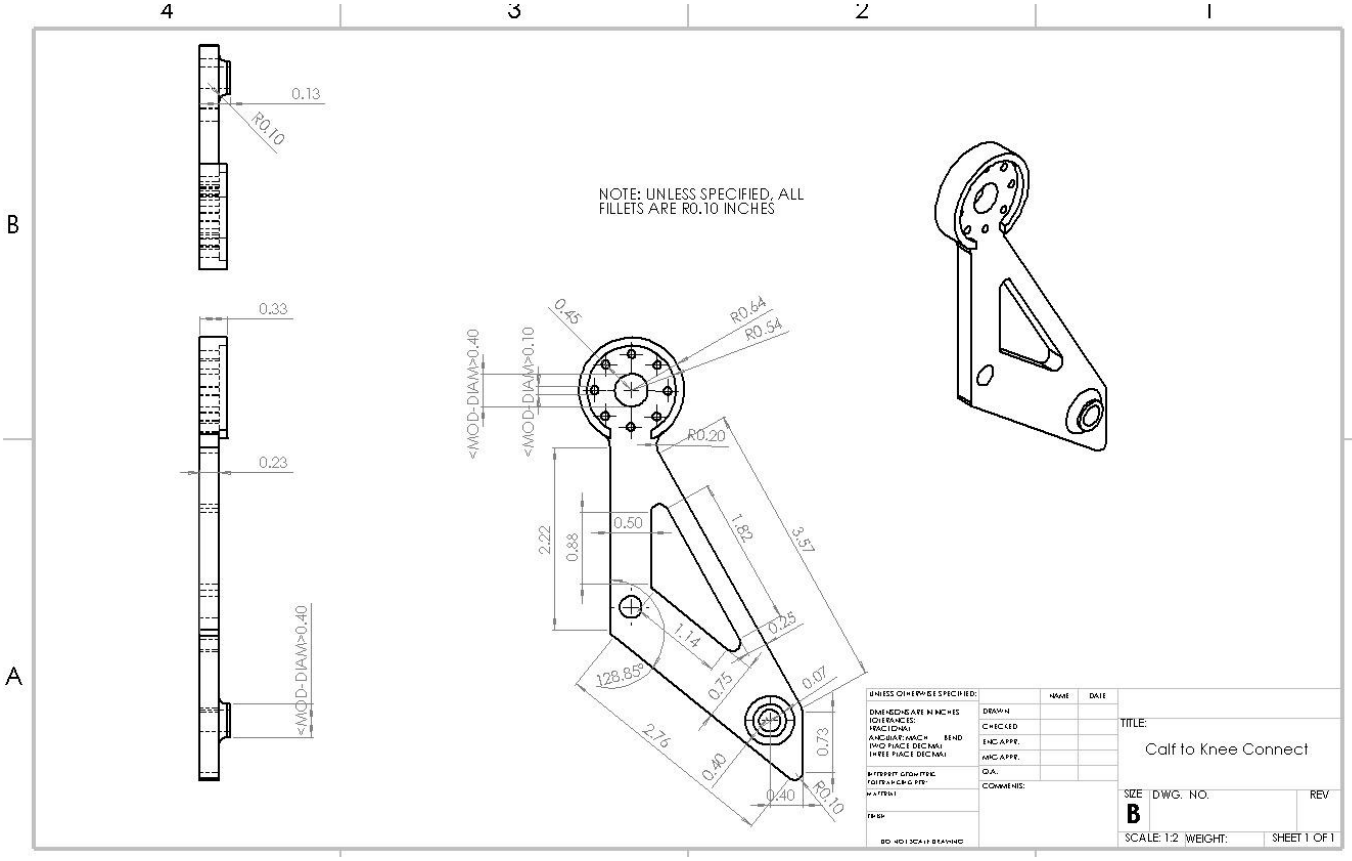
4
3
2
1
B
A
0.13
R0.10
0.33
0.23
<MOD-DIAM>0.40
NOTE: UNLESS SPECIFIED, ALL FILLETS ARE R0.10 INCHES
<MOD-DIAM>0.40
<MOD-DIAM>0.10
0.45
R0.64
R0.54
R0.20
2.22
0.88
0.50
1.82
3.57
1.14
0.25
128.85°
0.75
0.07
2.76
0.40
0.73
0.40
R0.10
UNLESS OTHERWISE SPECIFIED:
DIMENSIONS ARE IN INCHES
TOLERANCES:
FRACTIONAL
ANGULAR: MACH BEND
TWO PLACE DECIMAL
THREE PLACE DECIMAL
INTERPRET GEOMETRIC TOLERANCING PER:
MATERIAL
FINISH
DO NOT SCALE DRAWING
NAME
DATE
DRAWN
CHECKED
ENG APPR.
MFG APPR.
Q.A.
COMMENTS:
TITLE:
Calf to Knee Connect
SIZE
B
DWG. NO.
REV
SCALE: 1:2
WEIGHT:
SHEET 1 OF 1

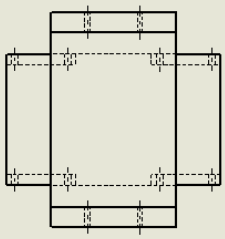

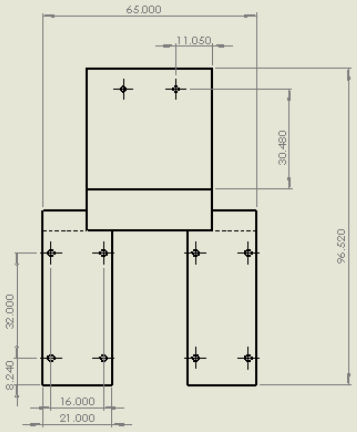

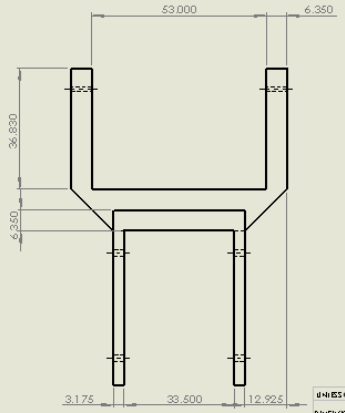

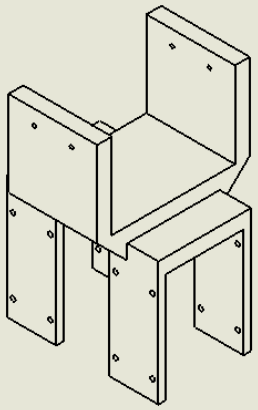

NOTE: PART IS SYMMETRIC
FRONT TO BACK AND RIGHT
TO LEFT

UNLESS OTHERWISE SPECIFIED:		NAME	DATE
DIMENSIONS ARE IN MILLIMETERS	DRAWN		
TOLERANCES:	CHECKED		
FRACTIONAL ±0.400 mm	ENG APPR.		
ANGULAR: MACH ±0.500 BEND ±1.000	MFG APPR.		
TWO PLACE DECIMAL ±0.250 mm			
THREE PLACE DECIMAL ±0.050 mm	Q.A.		
INTERPRET GEOMETRIC TOLERANCING PER:	COMMENTS:		
MATERIAL			
FINISH			
DO NOT SCALE DRAWING			

TITLE:

Hip Quad Bracket

SIZE	DWG. NO.	REV
B		

SCALE: 1:2 WEIGHT: SHEET 1 OF 1

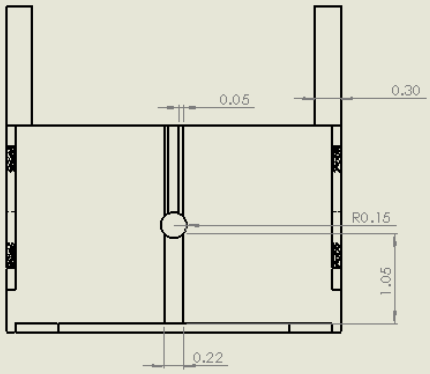

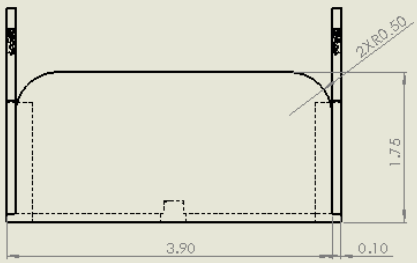

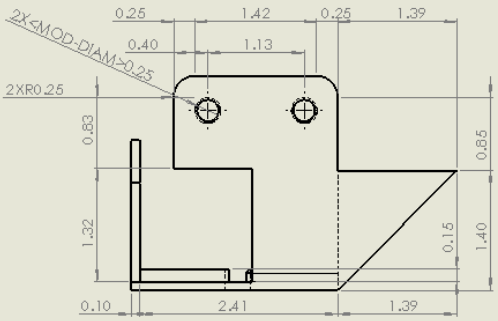

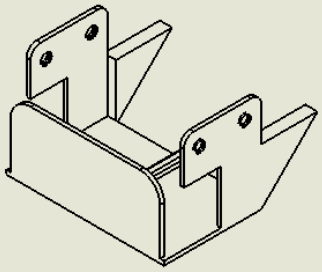

NOTE: PART IS SYMMETRIC
ABOUT CENTER AND HOLES
ARE TAPPED 1/4-20

UNLESS OTHERWISE SPECIFIED:		NAME	DATE
DIMENSIONS ARE IN INCHES	DRAWN		
TOLERANCES:	CHECKED		
FRACTIONAL	ENG APPR.		
ANGULAR: MACH BEND	MFG APPR.		
TWO PLACE DECIMAL			
THREE PLACE DECIMAL	Q.A.		
INTERPRET GEOMETRIC TOLERANCING PER:	COMMENTS:		
MATERIAL			
NEXT ASSY	USED ON		
APPLICATION	DO NOT SCALE DRAWING		

TITLE:

Quad Mount

SIZE	DWG. NO.	REV
B		

SCALE: 1:2 WEIGHT: SHEET 1 OF 1

Arm Drawings:

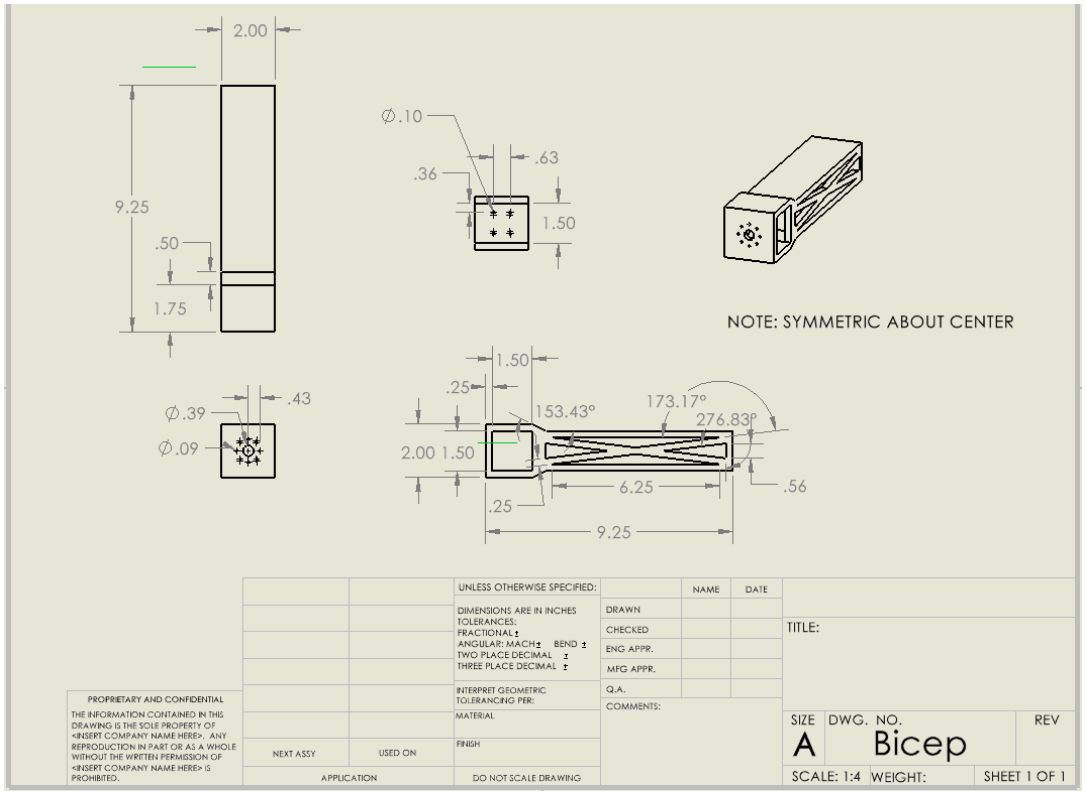

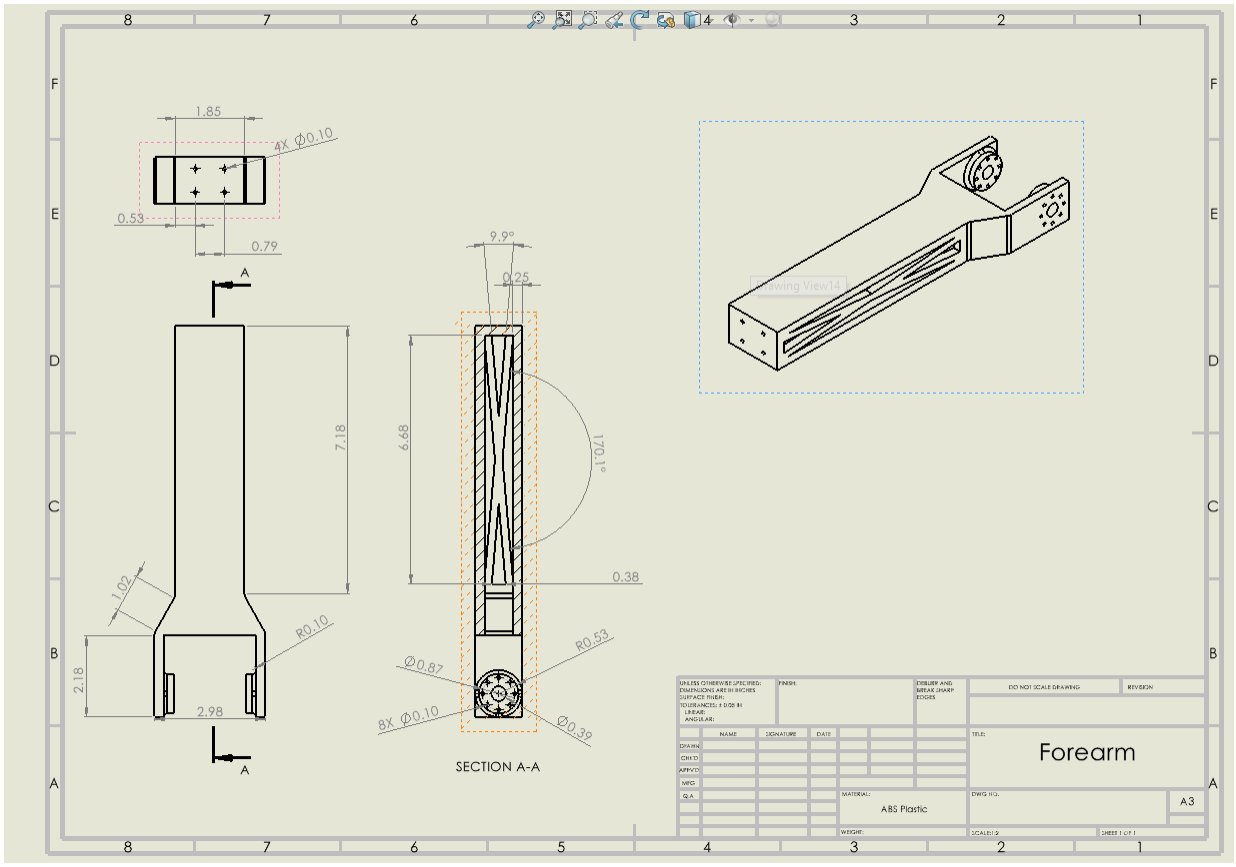

Original Hip Drawing**:**

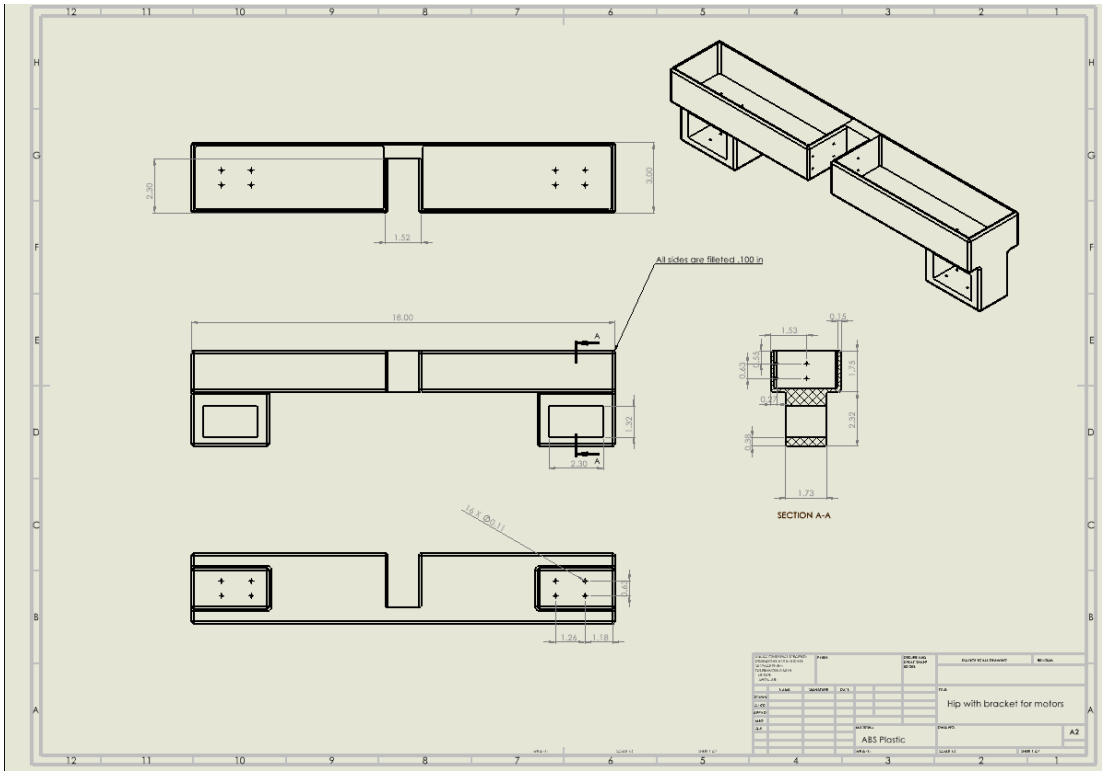

Updated Hip Drawing:

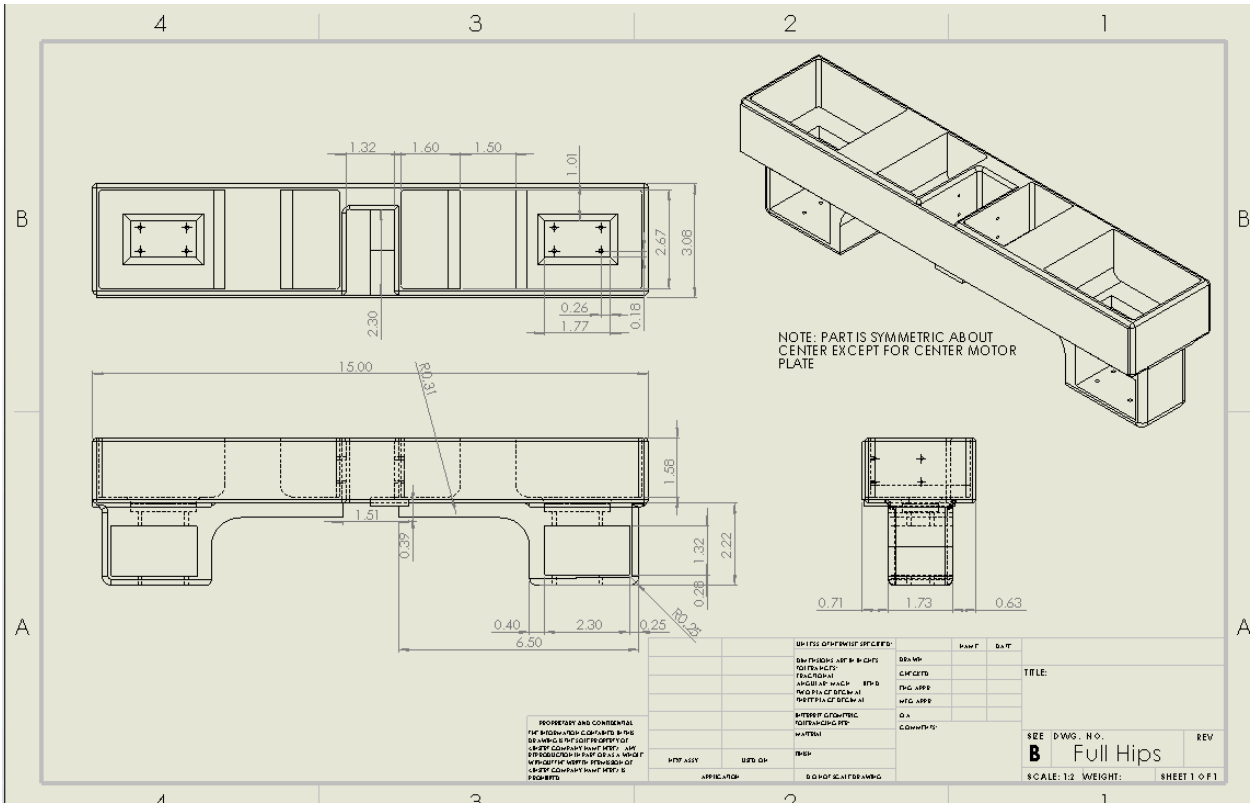

Shoulder Joint Drawing:

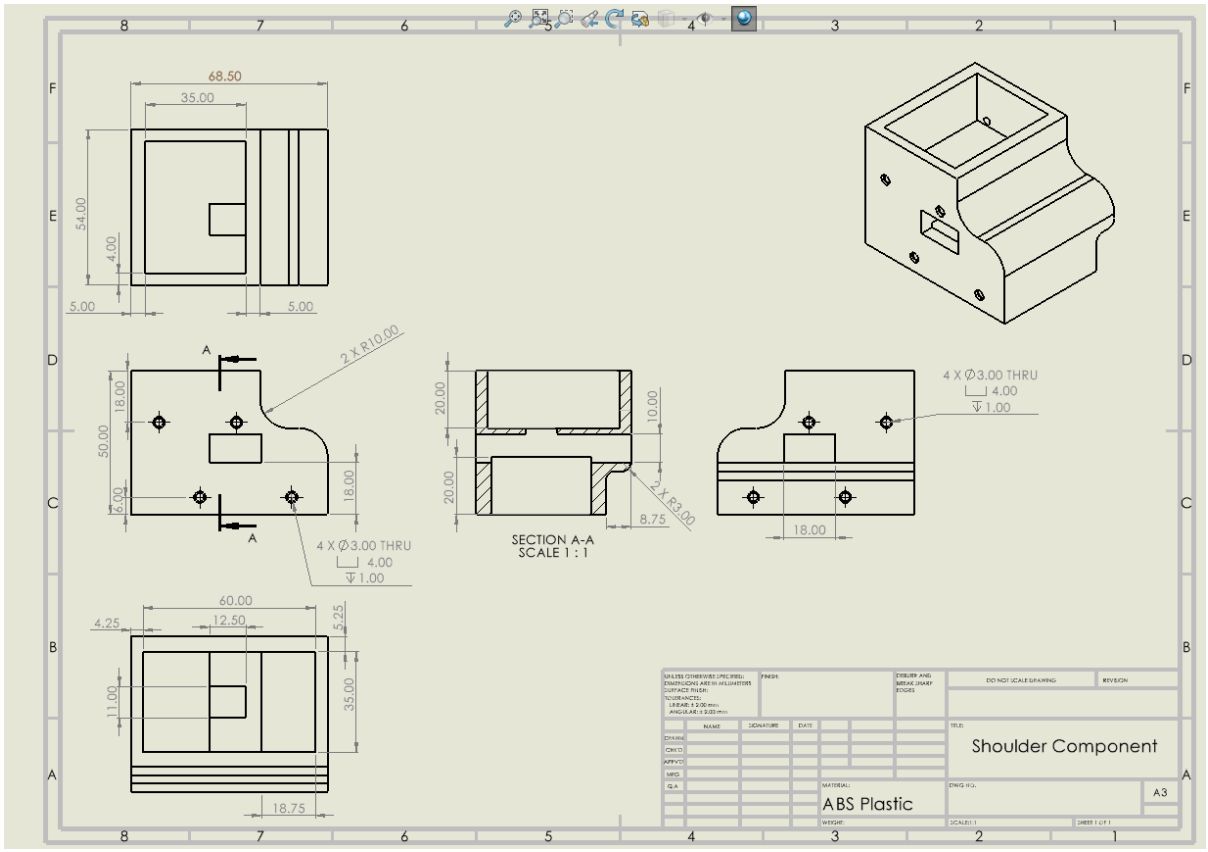

Torso Front:

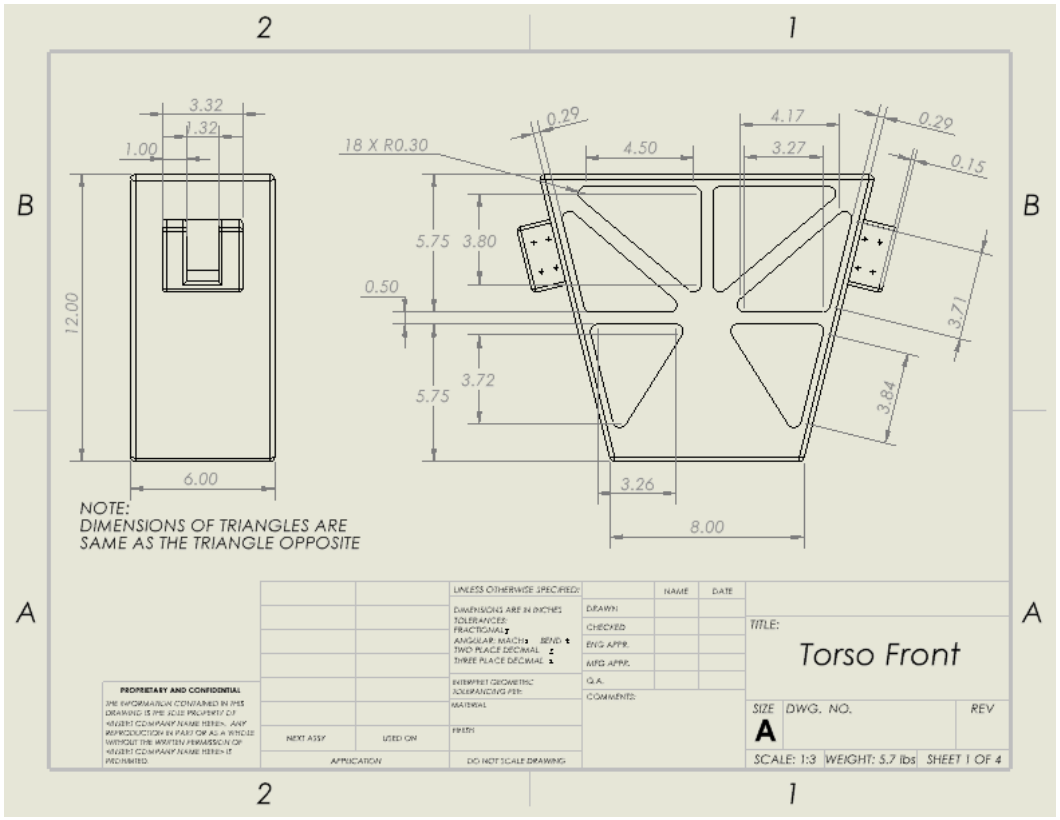

Torso Top View:

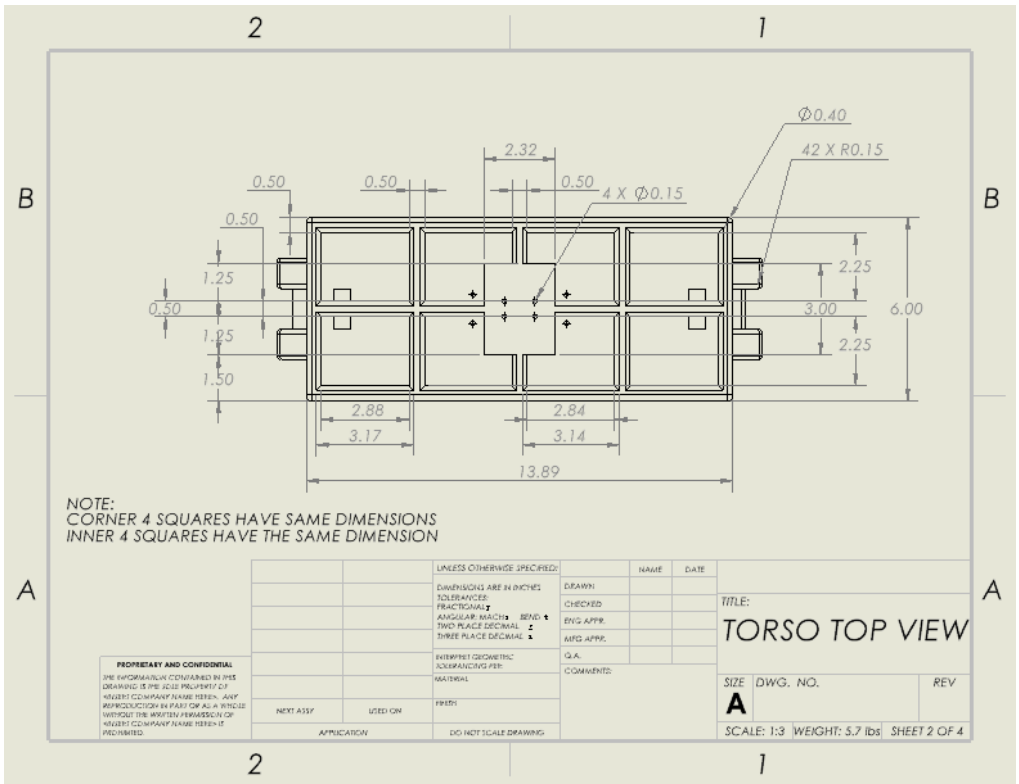

Torso to Arm Connection:

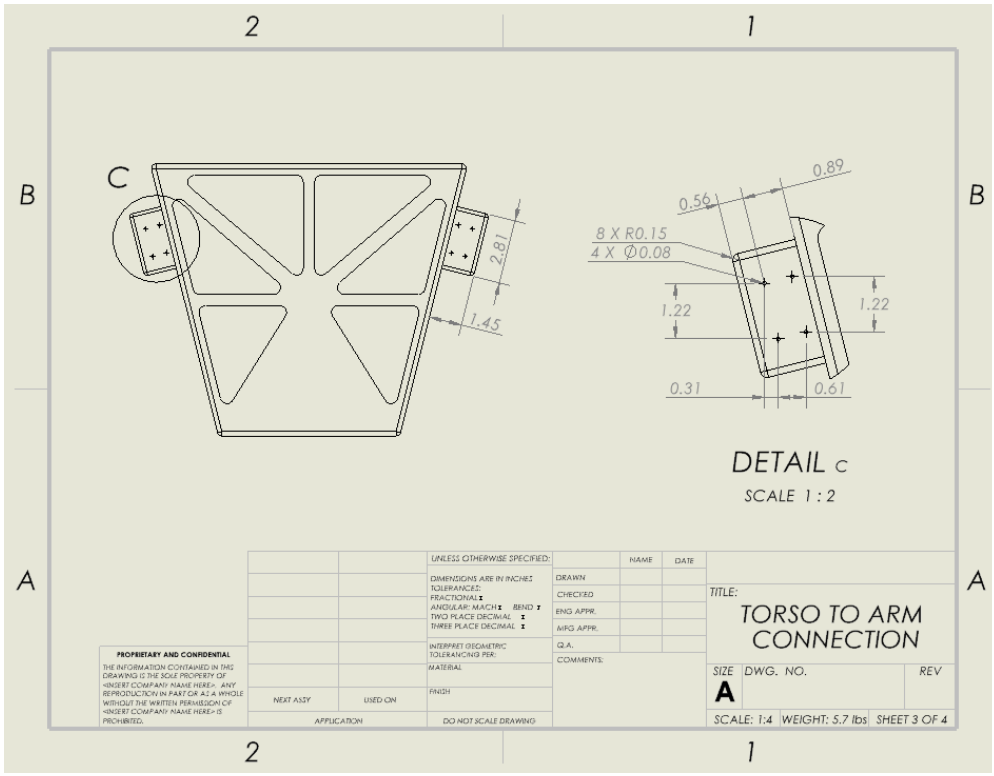

Torso Bottom View:

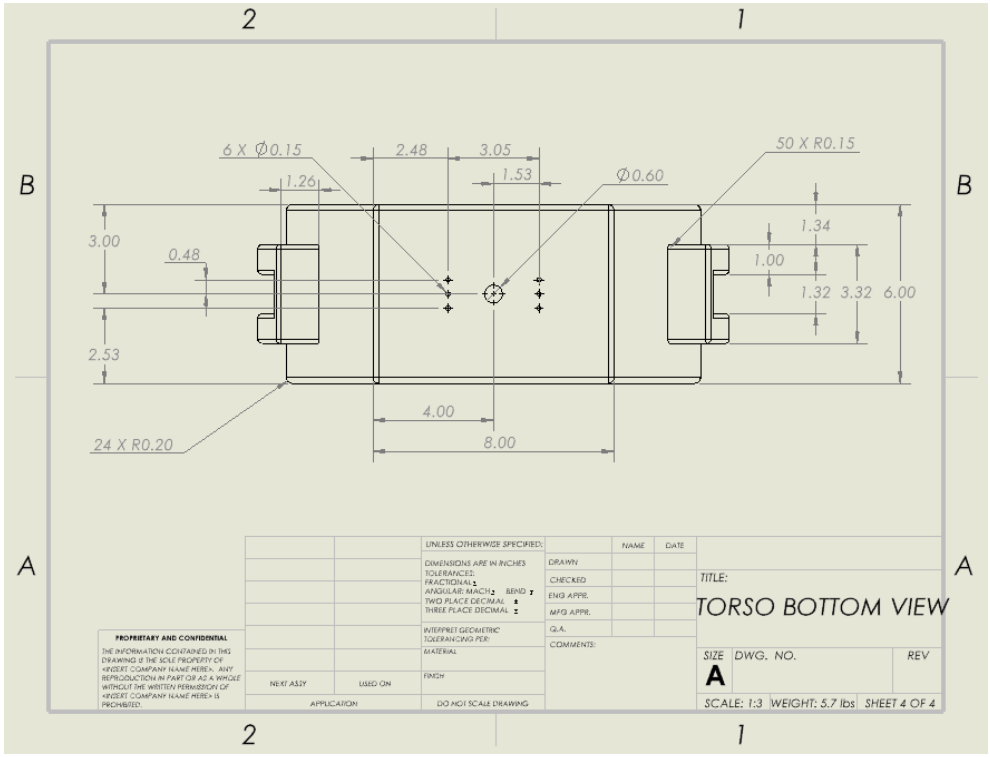

Spine Rod:

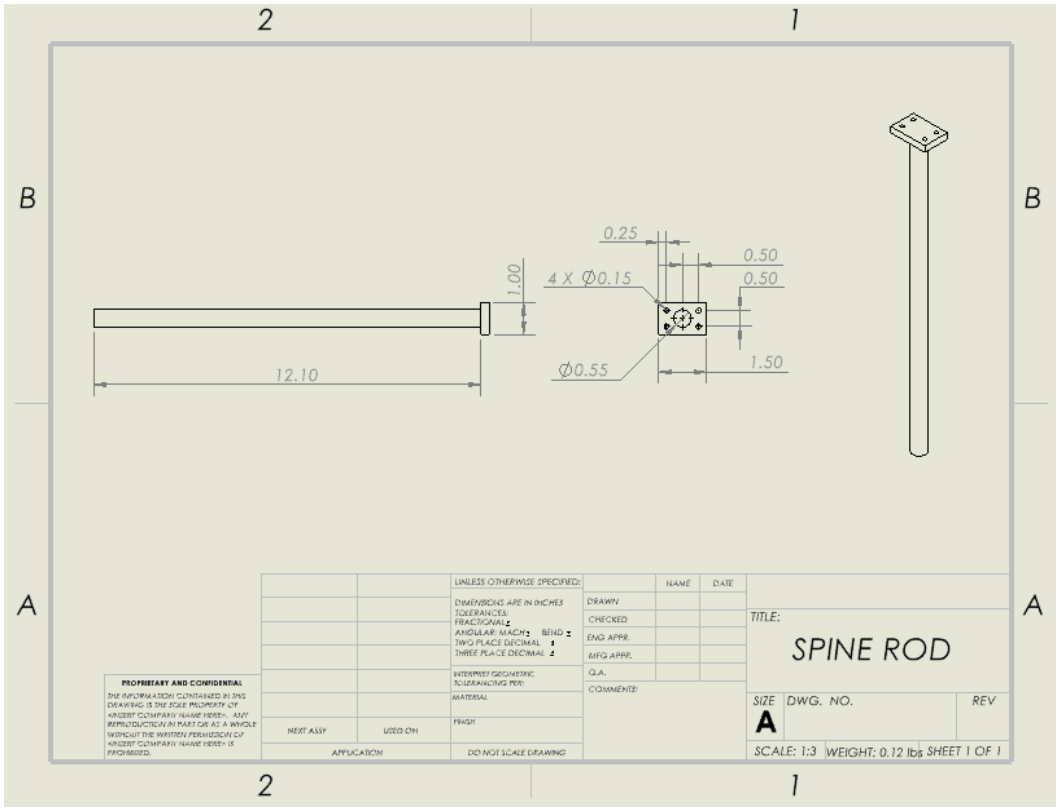

Motor to Torso Connector:

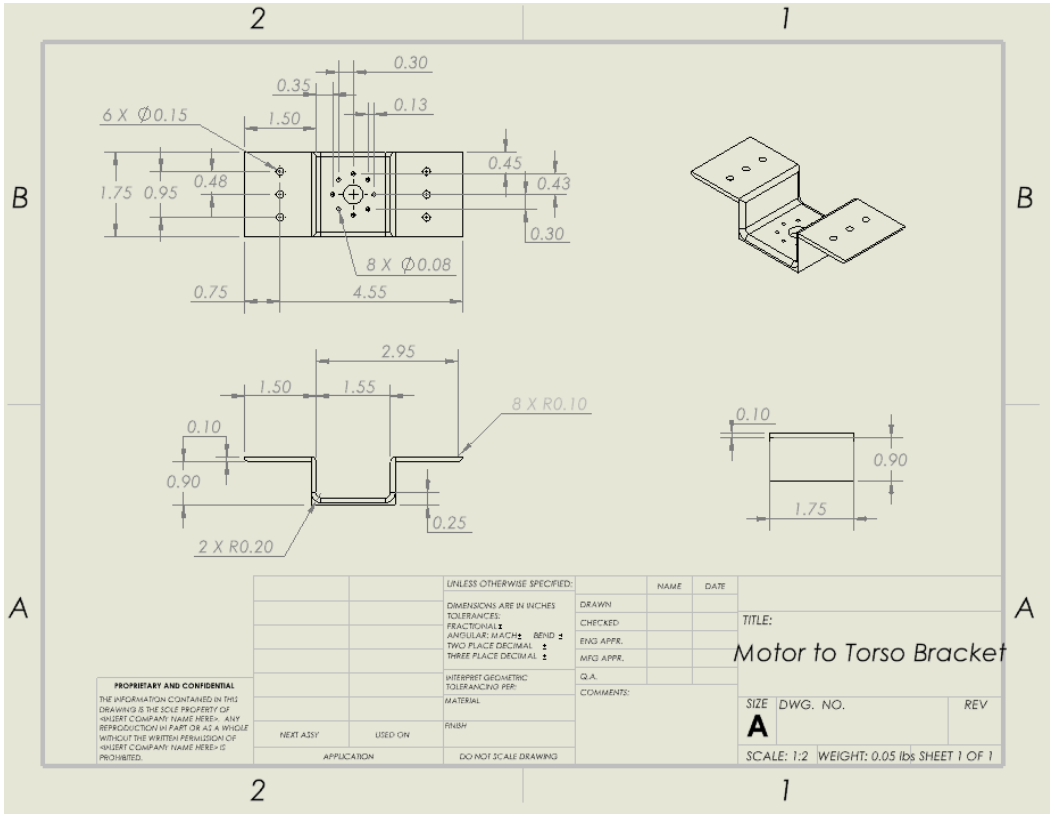

Appendix C: Bill of Materials

Component	Volume (mm^3)	Quantity	Net
Calf	392090.397	2	784180.8
Quad	619259.860	2	1238520
Rear Ankle Bracket	8666.666	2	17333.33
Front Ankle Bracket	14425.036	2	28850.07
Hip Quad Mount	62485.719	2	124971.4
Knee	46401.264	2	92802.53
Knee Motor Arm	3010.644	4	12042.58
Hips	580590.070	1	580590.1
Motor to Torso	19207.195	1	19207.2
Torso	2575952.665	1	2575953
Shoulder Block	109466.340	2	218932.7
Bicep	201918.270	2	403836.5
Forearm	193376.880	2	386753.8

Total Volume (mm^3)
6483973.372

Total Volume (cm^3)
6483.973372

Density of ABS (g/cm^3)
1.1

Mass of ABS Needed (g)
7132.37071

Rounded Up Per Print Total
8000

Volume estimate for the mass of ABS needed per robot calculation

Item	Price	Quantity	Link		Net Price	Total
10 kg ABS (White)	249.99	1	https://www.pushplastic.com/products/abs-filament-1-75mm-10kg?variant=44429614579873		249.99	1026.81
Leg Dampers	22.99	2	https://www.amazon.com/HLLions-Absorber-Internal-Crawler-Upgrade/dp/B07W1NGC3X/ref=asc_df_B07W1NGC3X/?tag=hyprod-20&linkCode=df0&hvadid=692875362841&hvpos=&hvnetw=g&hvrand=8203860332563476970&hvpone=&hvptwo=&hvqmt=&hvdev=c&hvdvcmdl=&hvlocint=&hvlocphy=1027070&hvtargid=pla-2281435178298&mcid=e85c3b92f9393b448de859181244c2ba&hvocijid=8203860332563476970-B07W1NGC3X-&hvexpln=73&th=1		45.98	
FR13-HK101K Set	66.7	8	https://www.robotis.us/fr13-h101k-set/		533.6	
FR13-S102K Set	27.4	2	https://www.robotis.us/fr13-s102k-set/		54.8	
Dynamixel XM540-270R	N/A	23	N/A			
1/4-20 X 1 Bolt Pack	12.36	1	https://www.mcmaster.com/91251A542/		12.36	
M2.5 X 14mm Bolt Pack	7.52	5	https://www.mcmaster.com/91290A053/		37.6	
M2.5 X 6mm Bolt Pack	11.56	8	https://www.mcmaster.com/91290A101/		92.48	

Bill of Materials